CERN-PH-EP/2014-303
2015/02/19

CMS-SMP-13-014

Measurement of the $Z\gamma$ production cross section in pp collisions at 8 TeV and search for anomalous triple gauge boson couplings

The CMS Collaboration*

Abstract

The cross section for the production of $Z\gamma$ in proton-proton collisions at 8 TeV is measured based on data collected by the CMS experiment at the LHC corresponding to an integrated luminosity of 19.5 fb^{-1} . Events with an oppositely-charged pair of muons or electrons together with an isolated photon are selected. The differential cross section as a function of the photon transverse momentum is measured inclusively and exclusively, where the exclusive selection applies a veto on central jets. The observed cross sections are compatible with the expectations of next-to-next-to-leading-order quantum chromodynamics. Limits on anomalous triple gauge couplings of $ZZ\gamma$ and $Z\gamma\gamma$ are set that improve on previous experimental results obtained with the charged lepton decay modes of the Z boson.

Submitted to the Journal of High Energy Physics

1 Introduction

The study of $Z\gamma$ production in proton-proton (pp) collisions at TeV energies represents an important test of the standard model (SM), which prohibits direct coupling between the Z boson and the photon. Within the SM $Z\gamma$ production is primarily due to radiation of photons from initial-state quarks (ISR) or final-state leptons (FSR). However, new physics phenomena at higher energies may be manifested as an effective self-coupling among neutral gauge bosons, resulting in a deviation from their predicted zero values in the SM. Models of anomalous triple gauge couplings (aTGC) have been introduced and discussed in Refs. [1–3].

This paper presents a measurement of $Z\gamma$ production in pp collisions at a center-of-mass energy of 8 TeV, based on data collected with the CMS experiment in 2012, corresponding to an integrated luminosity of 19.5 fb^{-1} . For this analysis the decays of the Z boson into a pair of muons ($\mu^+\mu^-$) or electrons (e^+e^-) are considered. The processes of ISR and FSR contribute to $\ell^+\ell^-\gamma$ ($\ell = \mu, e$) production in the SM at leading order (LO), and these are exemplified by the first two Feynman diagrams in Fig. 1. Photons can also be produced by jet fragmentation, but these photons are not considered as signal in the present analysis and are strongly suppressed by requiring that the photon is isolated. The production of $Z\gamma$ through triple gauge couplings is represented by the third diagram in Fig. 1.

Both ATLAS and CMS Collaborations have presented measurements of the inclusive $Z\gamma$ cross section and searches for anomalous $ZZ\gamma$ and $Z\gamma\gamma$ couplings using data collected at a center-of-mass energy of 7 TeV [4, 5]. The larger 2012 data sample and the increased cross section at 8 TeV allow for the first measurement of the inclusive differential cross section for $Z\gamma$ production as a function of the photon transverse momentum p_T^γ . Results on the differential $Z\gamma$ cross section for events with no accompanying central jets, referred to as exclusive cross sections, are also presented, providing some insight into the effect of additional jets on the distribution of p_T^γ . The cross sections are measured for photons with $p_T^\gamma > 15 \text{ GeV}$ and restricted to a phase space defined by kinematic requirements on the final-state particles that are motivated by the experimental acceptance. In addition, the photon is required to be separated from the leptons by $\Delta R(\ell, \gamma) > 0.7$ where $\Delta R = \sqrt{(\Delta\phi)^2 + (\Delta\eta)^2}$, ϕ is the azimuthal angle and η the pseudorapidity. Furthermore, the dilepton invariant mass is required to be above 50 GeV. With this selection the fraction of FSR photons is reduced and photons originating from ISR or aTGCs are dominant.

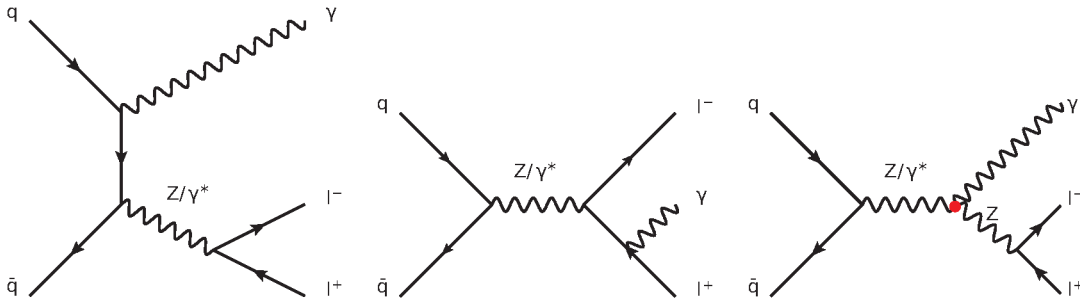


Figure 1: Leading-order Feynman diagrams for $Z\gamma$ production in pp collisions. Left: initial-state radiation. Center: final-state radiation. Right: diagram involving aTGCs that are forbidden in the SM at tree level.

2 The CMS detector and particle reconstruction

The central feature of the CMS apparatus is a superconducting solenoid of 6 m internal diameter, providing a magnetic field of 3.8 T. Within this superconducting solenoid volume are a silicon pixel and strip tracker, a lead tungstate crystal electromagnetic calorimeter (ECAL), and a brass and scintillator hadron calorimeter (HCAL), each composed of a barrel and two endcap sections. Muons are measured in gas-ionization detectors embedded in the steel flux-return yoke outside the solenoid. Extensive forward calorimetry complements the coverage provided by the barrel and endcap detectors.

The silicon tracker measures charged particles within the pseudorapidity range $|\eta| < 2.5$. The ECAL provides coverage in pseudorapidity $|\eta| < 1.479$ in a barrel region (EB) and $1.479 < |\eta| < 3.0$ in two endcap regions (EE). A preshower detector consisting of two planes of silicon sensors interleaved with a total of three radiation lengths of lead is located in front of the EE regions. Muons are measured in the pseudorapidity range $|\eta| < 2.4$, with detection planes made using three technologies: drift tubes, cathode strip chambers, and resistive-plate chambers.

The particle-flow (PF) algorithm [6–8] reconstructs and identifies each particle with an optimized combination of all subdetector information and categorizes reconstructed objects as photons, muons, electrons, charged hadrons, and neutral hadrons. The energy of photons is obtained from a cluster of energy depositions in ECAL crystals. The photon direction is determined by assuming it is associated to the main interaction vertex, defined as the vertex that has the highest value for the sum of p_T^2 of the associated tracks that is also compatible with the beam interaction point. The energy of electrons is determined from a combination of the track momentum at the main interaction vertex, the ECAL cluster energy, and the energy sum of all bremsstrahlung photons attached to the track [9, 10]. The energy of muons is obtained from the corresponding track momentum measured in the silicon tracker and the muon detection system. The energy of charged hadrons is determined from a combination of the track momentum and the corresponding ECAL and HCAL energies. Finally, the energy of neutral hadrons is obtained from the corresponding ECAL and HCAL energies.

Jets used for the exclusive measurement presented in this paper are reconstructed from PF objects, clustered by the anti- k_T algorithm [11, 12] with a distance parameter of 0.5. The measured jet momentum is the vectorial sum of all particle momenta in the jet and is found from the simulation to be within 5–10% [13] of the initial jet momentum over the whole p_T range and detector acceptance. An offset correction is applied to take into account the extra energy clustered in jets due to additional pp interactions within the same bunch crossing (pileup) [14].

A more detailed description of the CMS detector, together with a definition of the coordinate system used and the relevant kinematic variables, can be found in Ref. [15].

3 Signal and background modeling

Simulation samples for the signal process, $\ell^+ \ell^- \gamma + n$ partons ($n = 0, 1, 2$) at matrix element level are produced with the event generator SHERPA 1.4 [16] for the muon and electron channels separately. The cross sections are calculated at next-to-leading order (NLO) in quantum chromodynamics (QCD) using MCFM 6.4 [17] and the CT10 [18] parton distribution functions (PDF). Additional PDF sets are provided by CT10 to represent the uncertainties in the PDFs. These are used to estimate the PDF uncertainties in the cross sections following the prescription in Ref. [19]. The effect of using the CT10 PDF sets, where the value of the strong coupling constant α_s is varied in the fit, has been studied and is considered as an additional uncertainty.

The uncertainties from factorization, renormalization, and photon fragmentation scales are estimated by varying each of these scales up and down by a factor of two. The uncertainty in the exclusive cross section calculation is obtained by following the recommendation in Ref. [20] of adding in quadrature the scale uncertainties of the $\ell^+\ell^-\gamma$ NLO and the $\ell^+\ell^-\gamma + 1$ parton LO calculations. We also compare the measurement with a next-to-next-to-leading-order (NNLO) calculation of the inclusive cross section provided by Ref. [21].

The major sources of background to the $Z\gamma$ process are Drell–Yan (DY) + jets, WW , WZ , ZZ , and $t\bar{t}$ production. These are simulated with the MADGRAPH 4 [22] matrix element generator, using the CTEQ6L PDF set [23], and interfaced with PYTHIA 6.4.26 [24] to describe parton showers, fragmentation, and initial and final state radiation of photons. The cross sections for $t\bar{t}$ and diboson production are normalized to the NLO QCD calculation from MCFM. The DY+jets sample is normalized to the NNLO QCD calculation of FEWZ [25]. It is used to describe the background of nonprompt and misidentified photons. All events containing a prompt photon that passes the signal requirements are removed from this sample. The QCD simulation, which is used for the background determination, is produced using PYTHIA. All samples are passed through a detailed simulation of the CMS detector based on GEANT4 [26] and reconstructed using the same algorithms as used for data.

4 Event selection

The measurements presented in this paper rely on the reconstruction and identification of isolated muons, electrons, and photons. The exclusive cross section measurement is also dependent on the reconstruction of jets. Details of the identification and selection of muons (electrons) can be found in Ref. [27] (Ref. [28]).

Leptons from Z boson decays are typically isolated, i.e., separated in ΔR from other particles. A requirement on the lepton isolation is used to reject leptons produced in decays of hadrons. The muon isolation is based on tracks from the main interaction vertex as this is always identified as the source of the lepton pair. The isolation variable I_{trk} is defined as the p_T sum of all tracks except for the muon track originating from the main interaction vertex within a cone of $\Delta R(\mu, \text{track}) < 0.3$. The value of I_{trk} is required to be less than 10% of the muon p_T . For electrons the isolation variable is the p_T sum of neutral hadrons, charged hadrons, and photon-like PF objects in a cone of $\Delta R < 0.3$ around the electron. Contributions of the electron to the isolation variables are suppressed using a veto region. This isolation variable is required to be smaller than 10% (15%) of the electron p_T for electrons in the EB (EE). An event-by-event correction is applied, which keeps the selection efficiency constant as a function of pileup interactions [29].

Quality selection criteria are applied to the reconstructed photons to suppress the background from hadrons misidentified as photons. The ratio of the energy deposition in the HCAL tower behind the ECAL cluster to the energy deposition in the ECAL has to be below 5%. The background is further suppressed by a requirement on the shower shape variable $\sigma_{\eta\eta}$ [30], which measures the shower width along the η direction in a 5×5 matrix of crystals centered on the crystal of highest energy in the cluster. The electromagnetic shower produced by a photon is expected to have a small value of $\sigma_{\eta\eta}$. Therefore, a selection of $\sigma_{\eta\eta} < 0.011$ (0.033) in the EB (EE) region is applied. To suppress electrons misidentified as photons, photon candidates are rejected if measurements in the silicon pixel detector are found and these measurements are consistent with an electron, which is incident on the ECAL at the location of the photon cluster. The isolation variables based on PF charged hadrons I_c , neutral hadrons I_n , and photon objects I_γ are calculated as the sum of p_T in a cone of $\Delta R < 0.3$ around the photon. Contributions of the

photon itself are suppressed using a veto region. Again, the isolation values are corrected for the average energy deposition due to pileup. The isolation requirements used in the EB region are $I_n < 1.0 + 0.04p_T^\gamma$, $I_\gamma < 0.7 + 0.005p_T^\gamma$, and $I_c < 1.5$. In the EE region $I_n < 1.5 + 0.04p_T^\gamma$, $I_\gamma < 1.0 + 0.005p_T^\gamma$, and $I_c < 1.2$ are required.

Events are selected online using a dimuon or dielectron trigger with thresholds of $p_T > 17$ GeV for the leading and $p_T > 8$ GeV for the subleading lepton. Candidate events are required to have two same-flavor opposite-charge selected leptons and a selected photon. Muons with $|\eta| < 2.4$ relative to the main interaction vertex are selected, while electrons need to satisfy $|\eta_{SC}| < 1.44$ or $1.57 < |\eta_{SC}| < 2.5$, where η_{SC} is determined by the cluster position in the ECAL with respect to the center of the CMS detector. This excludes the transition region between EB and EE. The p_T of each lepton has to be greater than 20 GeV, and the dilepton mass $M_{\ell\ell}$ is required to be greater than 50 GeV. At least one photon candidate with $p_T^\gamma > 15$ GeV is required. The η range for photons is determined by the coverage of the ECAL and the silicon tracker and is the same as for electrons. The minimum distance between the photon and the leptons must be $\Delta R(\ell, \gamma) > 0.7$. In the very rare cases when a second photon is reconstructed, the photon with the higher p_T^γ is used for the differential cross section measurement.

A tag-and-probe method, similar to that presented in Ref. [31], is used to measure the lepton reconstruction efficiencies. The photon reconstruction efficiency is determined with a modified tag-and-probe method that makes use of the Z boson mass peak in the $M_{\mu\mu\gamma}$ distribution for FSR photons. Scale factors are obtained from the measured efficiencies to correct the simulation. In Fig. 2 the observed p_T^γ distribution and the invariant mass of the two leptons and the photon candidate $M_{\ell\ell\gamma}$ are compared to the SM expectation. The level of agreement is discussed in Section 5. The final cross section measurement, with the background estimate coming from data, indicates that the observed deviation in the p_T^γ distribution is due to the imperfect modeling of the DY+jets background in the simulation.

5 Background estimation

The dominant background for this measurement is DY+jets containing nonprompt photons, e.g., through π^0 or η decays, or hadrons misidentified as photons. A template method is used to estimate this background from data. This method relies on the power of an observable to discriminate between signal photons and background. The signal yield is obtained from a maximum-likelihood fit to the observed distribution of such an observable using the known distributions (“templates”) for signal photons and background.

The cross sections are measured with two different template observables. One template method uses the shower shape variable $\sigma_{\eta\eta}$. The separation between the two photons from the decay of light particles such as π^0 , albeit small, leads to a larger $\sigma_{\eta\eta}$ value than for single photons. The shower width of strongly interacting particles that mimic a photon signature also tends to be larger.

The other template observable is $I_{\gamma,\text{nfp}}$, which is the p_T sum of all PF photon objects in a cone of $\Delta R < 0.4$ around the photon. The abbreviation “nfp” stands for “no footprint of the photon” and indicates the removal of energy associated with the photon from the isolation variable. This energy is removed by excluding all particles whose ECAL clusters overlap with the photon cluster from the isolation variable. This makes $I_{\gamma,\text{nfp}}$, and hence the signal template, independent of p_T^γ . Since the background particles are often produced in cascade decays, $I_{\gamma,\text{nfp}}$ for them is expected to be greater on average than for signal photons.

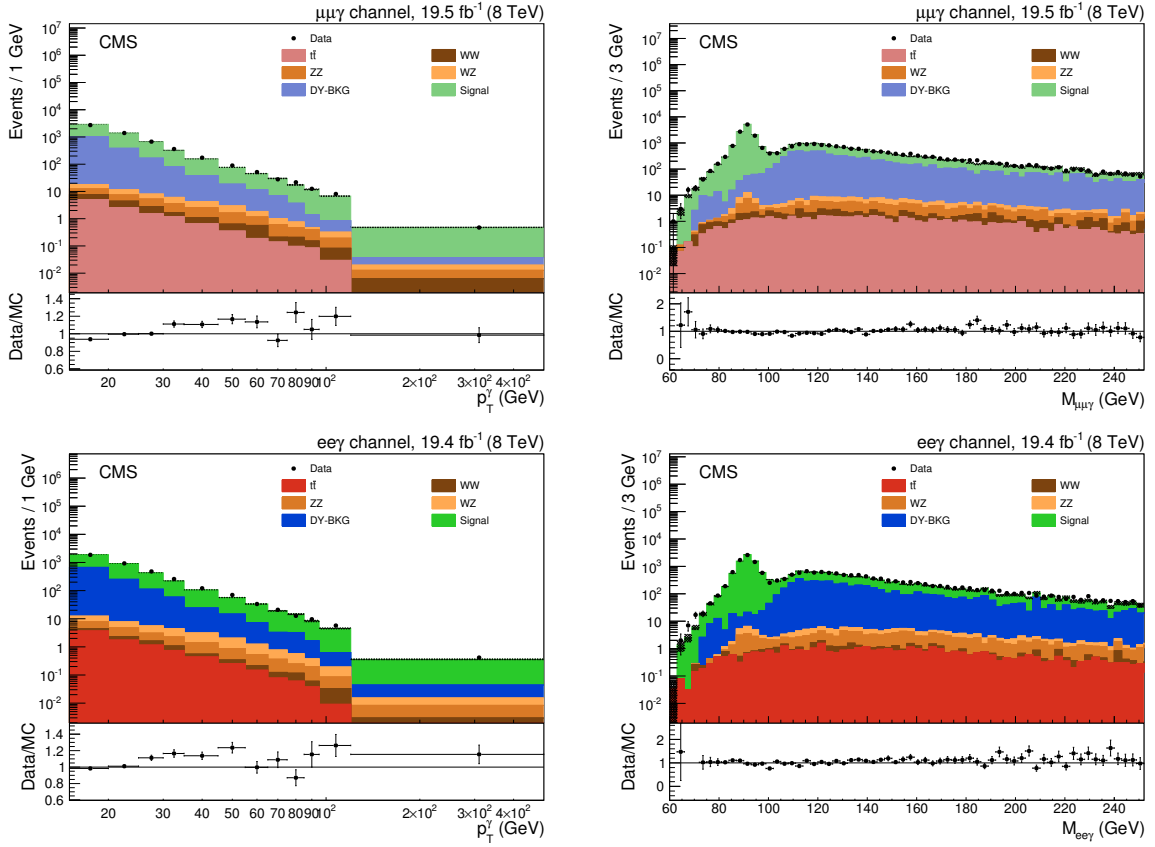


Figure 2: Left: p_T^γ distribution after the full event selection compared to the SM prediction. Right: the distribution of the invariant mass $M_{\ell\ell\gamma}$. The mass distribution has a peak at the Z boson mass, which arises from FSR photons. Events with ISR photons appear in the large tail above the Z boson mass where a large fraction of background is expected. The displayed uncertainties include only the statistical uncertainties in data and simulated samples.

5.1 Extraction of signal and background templates

The signal templates for both template variables are taken from data. A sample of photons with a background contamination of less than 1% is obtained from FSR $Z\gamma$ events. About 23 thousand photon candidates close to one of the leptons, with $0.3 < \Delta R(\ell, \gamma) < 0.8$, are selected. The minimum separation is chosen to reduce the influence of the lepton on the template variables. The invariant dilepton mass is selected to be between 40 and 80 GeV. One lepton is required to have a $p_T > 30$ GeV while for the other lepton only $p_T > 10$ GeV is required. All photon quality requirements are applied except for $\sigma_{\eta\eta}$, which cannot be used in the photon selection for the $\sigma_{\eta\eta}$ template method. For the $I_{\gamma, \text{nfip}}$ template method the selection on I_γ is not applied since the two variables are strongly correlated.

Different templates are chosen for the EB and EE regions, as well as for the lower p_T^γ bins of the cross section measurement. Due to the limited number of photons a common template is used for $p_T^\gamma > 35$ GeV. The uncertainties in the signal templates are discussed in Section 5.2.

For the background templates it is almost impossible to find a sample of nonprompt or misidentified photons that is free of signal-like prompt photons. Therefore, we choose a jet data sample where such background objects are enhanced. From this sample events with two leading hadronic jets with $p_T > 30$ GeV and no isolated muon or electron are selected. Additionally, we require a photon candidate with a minimum separation from the jets of $\Delta R(\gamma, \text{jet}) > 0.7$.

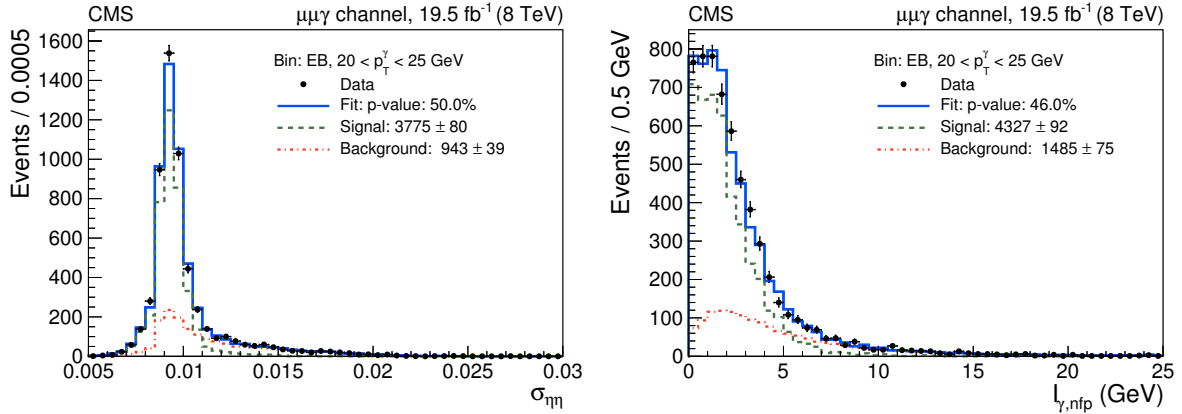


Figure 3: Fits of the $\sigma_{\eta\eta}$ templates (left) and the $I_{\gamma, \text{nfp}}$ templates (right) to the data for $20 < p_T^\gamma < 25 \text{ GeV}$ in the EB region. The extracted signal contributions are indicated by the green curves and the background contributions by the red ones.

Kinematic distributions of the jets and the photon candidates as well as the distributions of the photon selection variables in the jet data sample are well described by the QCD simulation. This agreement allows us to establish a selection of photon candidates for the background template using the QCD simulation and to apply the same selection on the jet data sample. This selection is required to be dominated by nonprompt and misidentified photon candidates whose template shape is in agreement with the background template prediction from the DY+jets simulation. When defining the selection for the $\sigma_{\eta\eta}$ background template, the photon candidates in the QCD simulation have to pass the full selection except for the requirements on $\sigma_{\eta\eta}$ and I_c . Starting from this preselection, the lower and upper boundaries on I_c are varied until a selection is found for which the template shape agrees with that in the DY+jets simulation. Once the selection is defined, it is applied to the jet data sample to obtain the $\sigma_{\eta\eta}$ background template that is used for the signal extraction.

The same method is used to find an $I_{\gamma, \text{nfp}}$ background template. In this case, the photon preselection in the QCD simulation does not include the requirements on $\sigma_{\eta\eta}$ and I_γ . Here the lower and upper boundaries on $\sigma_{\eta\eta}$ are varied to find an appropriate selection for a $I_{\gamma, \text{nfp}}$ background template.

We use these methods to obtain background templates from the data for the various p_T^γ bins in the EB and EE regions. The two different, almost uncorrelated, template variables are used for the cross section measurement and their results are compared. The methods rely on the DY+jets simulation, which is used to find the optimal background template selections. Hence, the agreement of the two methods provides an important consistency check. The uncertainties in these methods are discussed in Section 5.2.

5.2 Signal extraction

Using the templates obtained from the procedure described above the number of signal events is extracted in twelve p_T^γ bins, separately for the EB and EE. Examples of these binned maximum-likelihood fits are shown in Fig. 3. For the $\sigma_{\eta\eta}$ template method the $\sigma_{\eta\eta}$ requirement of the photon selection is applied after the fit. For the $I_{\gamma, \text{nfp}}$ template method the selection on I_γ cannot be applied on the binned data after the fit. Consequently, the photon selection efficiencies are different for the two methods. Therefore, we should not expect the same number of signal and background events before corrections for the efficiencies are applied.

The following sources of uncertainties are considered for the signal extraction:

- The statistical uncertainty in the signal templates due to the limited number of FSR photons available in data results in an uncertainty of 0.5–2% (EB) and 0.5–9% (EE) in the extracted signal yield that increases from low to high p_T^γ .
- The systematic uncertainty in the signal templates due to contamination of the FSR sample and the usage of a common template for all bins with $p_T^\gamma > 35$ GeV is estimated using the simulation. The uncertainties are 0.5–3% (EB) and 0.5–12% (EE) in the signal yield increasing from low to high p_T^γ .
- The number of events available in the DY+jets simulation that are used to find the appropriate selection for the background templates is low, especially in bins at high p_T^γ . The uncertainty in the extracted signal yield due to this limited sample size is 0.6–3% (EB) and 1.6–5% (EE) increasing from low to high p_T^γ .
- The agreement of the QCD simulation and jet data sample is essential for the background template determination. We evaluate the uncertainty due to this imperfect modeling by calculating the standard deviation of the difference between the signal fraction obtained with template fits in data and simulation for a large number of different background template selections each defined by certain lower and upper boundaries on the template selection variable, I_c for the $\sigma_{\eta\eta}$ templates and $\sigma_{\eta\eta}$ for the $I_{\gamma,\text{nfp}}$ templates. For data the background templates are taken from the jet data sample and for simulation from the QCD simulation sample. The uncertainty is estimated to be 0.3–6% (EB) and 3–6% (EE) increasing from low to high p_T^γ .
- The statistical uncertainty in the signal yield obtained from the template fit is very similar for the two methods and amounts to 2–9% (EB) and 3–14% (EE) increasing from low to high p_T^γ .

Additionally, we have to consider the small fraction of irreducible background events from $t\bar{t}$, ZZ, ZW, and WW production. These background yields are estimated from the SM simulation and subtracted from the p_T^γ distribution of signal candidates. At low p_T^γ this contribution is negligible compared to the background from nonprompt or misidentified photons. At higher p_T^γ the fraction of irreducible background events is less than 4%, which is small compared to the overall uncertainty of the measurement. Since these backgrounds are very small their uncertainties have a negligible effect on the measurement.

6 Cross section measurement

We measure the cross section for a phase space region that corresponds closely to that used for the event selection. This phase space is defined by several kinematic requirements on the final-state particles: the leptons from the Z boson decay need to satisfy $p_T > 20$ GeV and $|\eta| < 2.5$, and the dilepton mass has to be greater than 50 GeV. The photon is required to have $|\eta| < 2.5$ and needs to be separated from both leptons by $\Delta R(\ell, \gamma) > 0.7$. Finally, a requirement is put on the photon isolation at the generator level $I_{\text{gen}} < 5$ GeV to exclude photons from jet fragmentation. The isolation variable uses a cone size of $\Delta R < 0.3$ and sums the transverse momentum of partons in the case of MCFM and of final-state particles in the case of SHERPA. It has been verified with SHERPA that photons that do not pass the I_{gen} selection also fail to pass the photon selection at the detector level. The definition of the phase space for the cross section measurements is summarized in Table 1.

The procedure for extracting the differential cross section from the number of observed sig-

nal events involves two steps. First, we extract the number of events produced in each p_T^γ bin within a phase space defined by the requirements in Table 1 and the additional experimental requirements on η and η_{SC} as described in Section 4. The number of observed signal events needs to be corrected for detector effects. These include efficiencies as well as bin migrations due to resolution and energy calibration. Both effects are treated using unfolding techniques. For the unfolding the method of D’Agostini [32], as implemented in the ROOUNFOLD [33] software package, is used. The response matrices are obtained from the signal simulation. A different response matrix is required for the two template methods because of the different photon selections. After the unfolding, compatible signal yields are obtained with the two template methods. Bias and variance of the unfolding procedure are estimated using pseudo-experiments. The uncertainties in the unfolding are 1% at low p_T^γ increasing up to 6% for the high- p_T^γ bins. To estimate the effect of the uncertainties in the photon energy scale and resolution, the unfolding of the data is repeated varying the photon energy scale and resolution in the response matrix within one standard deviation. The observed effect on the unfolded event yield is about 2.4% and is almost independent of p_T^γ .

The second step is to extrapolate the unfolded event yield in each p_T^γ bin to the desired phase space taking into account the detector acceptance, which is calculated using MCFM (NLO) and verified with SHERPA. About 92% of the muon channel events and 87% of the electron channel events are within the detector acceptance. These values are only slightly p_T^γ dependent.

Table 1: Phase space definition of the $Z\gamma$ cross section measurements.

Cross section phase space
$M_{\ell\ell} > 50 \text{ GeV}$
$\Delta R(\ell, \gamma) > 0.7$
photon: $ \eta < 2.5, I_{\text{gen}} < 5 \text{ GeV}$
leptons: $ \eta < 2.5, p_T > 20 \text{ GeV}$

6.1 The inclusive cross section

The cross sections are calculated from the unfolded number of signal events N_i and the detector acceptance A_i in each p_T^γ bin using the relation $\sigma_i = N_i / (A_i L)$ with an integrated luminosity of $L = 19.5 \pm 0.5 \text{ fb}^{-1}$ for the muon channel and $L = 19.4 \pm 0.5 \text{ fb}^{-1}$ for the electron channel. The cross section values obtained with the two template methods are compatible within their uncertainties as shown in Fig. 4 (left). The correlation between the template variables $\sigma_{\eta\eta}$ and $I_{\gamma, \text{nfp}}$ is less than 30%. The compatibility of the two results is a good indication that the background estimation is correct. The correlation of 30% is also assumed for the uncertainties in the background subtractions with the two template methods. All other uncertainties, i.e., in the dilepton (2%) and photon (2%) efficiencies, the photon energy scale and resolution (2.4%), unfolding (1–6%), luminosity (2.6%), and statistical uncertainties are assumed to be 100% correlated between the two template methods. Since the two template methods show good agreement, the results are combined using the best linear unbiased estimator (BLUE) method [34], which takes into account the correlation of all uncertainties.

The combined results of the two template methods for the muon and the electron channels are, as expected from lepton universality, fully compatible as presented in Fig. 4 (right). For $p_T^\gamma > 15 \text{ GeV}$ inclusive cross sections of $2066 \pm 23 \text{ (stat)} \pm 97 \text{ (syst)} \pm 54 \text{ (lumi)} \text{ fb}$ and $2087 \pm$

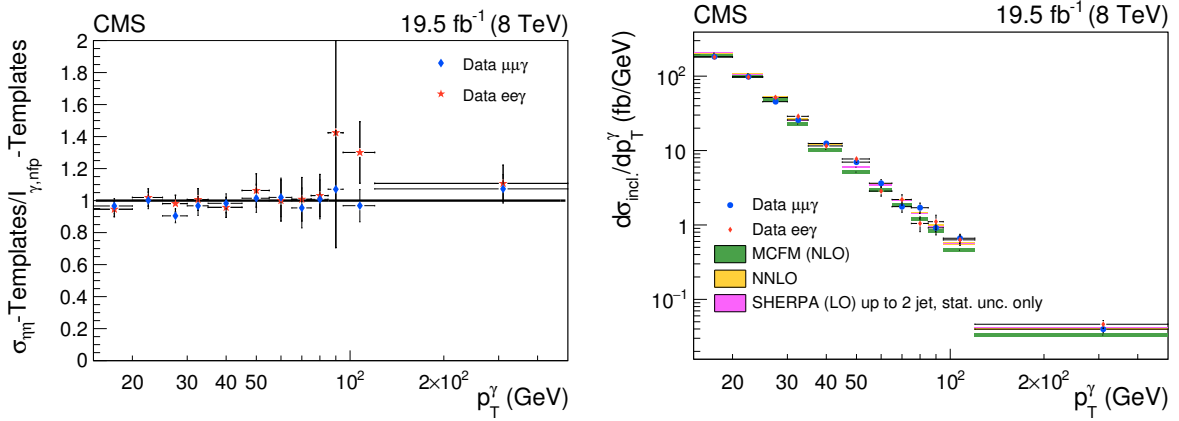


Figure 4: Left: ratio of the inclusive cross sections as obtained with the two template methods. Right: measured differential cross sections for the muon and electron channels using a combination of the two template methods compared to the NNLO [21], the MCFM (NLO) and the SHERPA SM predictions. The last bin is computed for the interval 120–500 GeV.

$30 \text{ (stat)} \pm 104 \text{ (syst)} \pm 54 \text{ (lumi)} \text{ fb}$ are measured for the muon and electron channels, respectively. The cross sections are combined using the BLUE method [34], assuming that the systematic uncertainties between the two lepton channels are highly correlated, since the signal yields are extracted using the same template shapes. The combined cross sections for the two channels are given in Table 2 and shown as the differential cross section in Fig. 5. It is compared to the MCFM (NLO), the NNLO, and the SHERPA predictions. For $p_T^\gamma > 15 \text{ GeV}$ the inclusive cross section is measured to be

$$\sigma_{\text{incl}} = 2063 \pm 19 \text{ (stat)} \pm 98 \text{ (syst)} \pm 54 \text{ (lumi)} \text{ fb.}$$

This is in good agreement with the MCFM prediction of $\sigma_{\text{incl}}^{\text{MCFM}} = 2100 \pm 120 \text{ fb}$ and the NNLO calculation [21] of $\sigma_{\text{incl}}^{\text{NNLO}} = 2241 \pm 22 \text{ (scale only)} \text{ fb}$. However, the ratio plot in Fig. 5 shows that at high p_T^γ the measurement is better described by the NNLO calculation and by SHERPA than by MCFM. The SHERPA calculation includes up to two partons in the matrix element which leads to a significant enhancement at high p_T^γ .

6.2 The exclusive cross section

To understand the effect of additional jets a measurement of the exclusive cross section is performed for $Z\gamma$ production without any accompanying jet with $p_T > 30 \text{ GeV}$ and $|\eta| < 2.4$.

The high instantaneous luminosity in the 2012 run requires that special care must be taken to reduce the contribution from jets produced in pileup interactions. About 50% of these jets can be rejected by requiring a maximal p_T fraction of charged particles in a jet originating from a pileup vertex. Further corrections are needed to account for the remaining contribution from pileup jets and jet reconstruction inefficiencies. The jet reconstruction efficiencies and jet misidentification rates for each p_T^γ bin are taken from the simulation where the jet misidentification rate considers all jets that cannot be matched to a jet from the main interaction at generator level. These are used to calculate the number of exclusive events from the measured number of inclusive events and the measured number of events with zero reconstructed jets. The latter are determined with the same methods used for the extraction of the inclusive signal yield. The uncertainties in the cross section due to pileup and jet energy scale are evaluated to be 1% and 2.5% respectively.

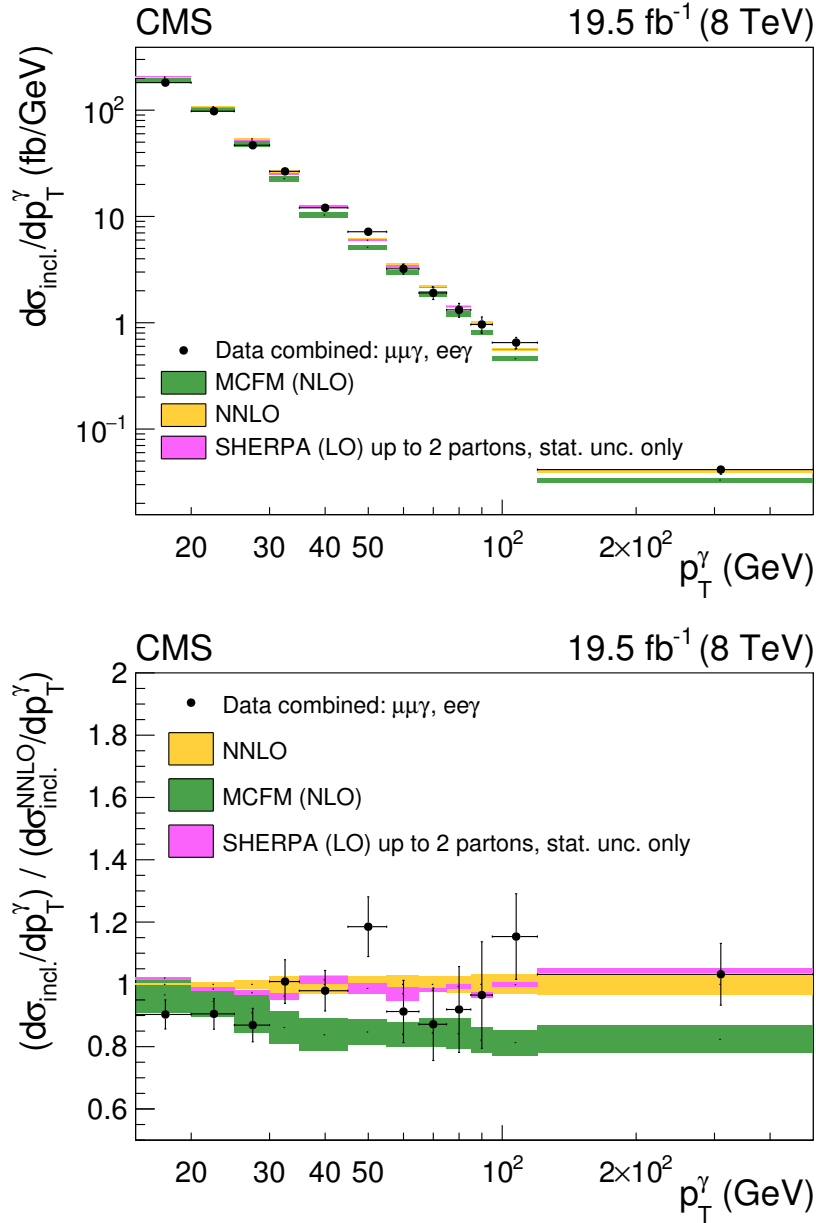


Figure 5: Top: combined inclusive differential cross section for the two lepton channels compared to the NNLO [21], the MCFM (NLO) and the SHERPA SM predictions. The latter is normalized to the NNLO cross section. The last bin is computed for the interval 120–500 GeV. Bottom: the ratios of the data and the other predictions to the NNLO calculation showing the effect of the additional partons on the inclusive cross section.

Table 2: The combined inclusive cross sections for the muon and electron channels with statistical, systematic, and integrated luminosity uncertainties, respectively. Scale and PDF uncertainties are included in the systematics for the MCFM (NLO) cross section calculation. Only scale uncertainties are considered for the NNLO calculation.

p_T^γ (GeV)	σ_{incl} (fb)	$\sigma_{\text{incl}}^{\text{MCFM}}$ (fb)	$\sigma_{\text{incl}}^{\text{NNLO}}$ (fb)
15–20	$908 \pm 12 \pm 39 \pm 24$	972 ± 57	1005.6 ± 2.6
20–25	$489 \pm 9 \pm 21 \pm 13$	510 ± 27	540.1 ± 3.7
25–30	$234 \pm 7 \pm 11 \pm 6$	245 ± 17	269.2 ± 3.6
30–35	$132.8 \pm 4.8 \pm 7.0 \pm 3.5$	113.4 ± 6.8	131.6 ± 3.5
35–45	$120.7 \pm 4.0 \pm 6.2 \pm 3.1$	103.2 ± 6.4	123.2 ± 3.6
45–55	$71.8 \pm 3.0 \pm 4.6 \pm 1.9$	51.3 ± 2.5	60.6 ± 1.6
55–65	$32.2 \pm 2.3 \pm 2.5 \pm 0.8$	29.6 ± 1.4	35.2 ± 1.0
65–75	$19.1 \pm 1.8 \pm 1.7 \pm 0.5$	18.5 ± 1.0	21.89 ± 0.56
75–85	$13.2 \pm 1.5 \pm 1.2 \pm 0.3$	12.10 ± 0.70	14.38 ± 0.38
85–95	$9.6 \pm 1.2 \pm 1.2 \pm 0.3$	8.19 ± 0.41	9.98 ± 0.31
95–120	$16.3 \pm 1.3 \pm 1.4 \pm 0.4$	11.47 ± 0.57	14.10 ± 0.44
>120	$15.8 \pm 1.0 \pm 1.0 \pm 0.4$	12.59 ± 0.68	15.29 ± 0.51

The p_T^γ distribution of exclusive events is unfolded and the cross sections are calculated. The acceptance is taken from MCFM (NLO). As shown in Fig. 6 (left) the results of the two template methods agree well and are combined using the BLUE method. With the requirement of $p_T^\gamma > 15$ GeV for the muon and the electron channels exclusive cross sections of 1774 ± 23 (stat) ± 115 (syst) ± 46 (lumi) fb and 1791 ± 29 (stat) ± 122 (syst) ± 47 (lumi) fb are measured, respectively. These and the differential cross sections presented in Fig. 6 (right) are compatible. The combined cross sections for the two channels are shown in Fig. 7.

The difference at high p_T^γ between the MCFM (NLO) calculation and SHERPA with up to two partons is smaller for the exclusive calculation. Currently there is no exclusive NNLO calculation available to be compared with the measurement. The measured cross section values are in agreement with the two available predictions. The combination of the two lepton channels compared to MCFM (NLO) is presented in Table 3 and the differential cross section is shown in Fig. 7. The ratio of the exclusive and inclusive cross sections is shown in Fig. 8. The fraction of exclusive events decreases with increasing p_T^γ and the fraction of events with additional jets changes from 10% to 40%. Adding the exclusive cross sections in all bins we obtain for $p_T^\gamma > 15$ GeV

$$\sigma_{\text{excl}} = 1770 \pm 18 \text{ (stat)} \pm 115 \text{ (syst)} \pm 46 \text{ (lumi)} \text{ fb.}$$

This is compatible with the MCFM (NLO) prediction of $\sigma_{\text{excl}}^{\text{MCFM}} = 1800 \pm 120$ fb.

7 Limits on aTGCs

The $ZZ\gamma$ or $Z\gamma\gamma$ aTGCs are formulated in the framework of an effective field theory considering dimension six and eight operators, that fulfill the requirements of Lorentz invariance and

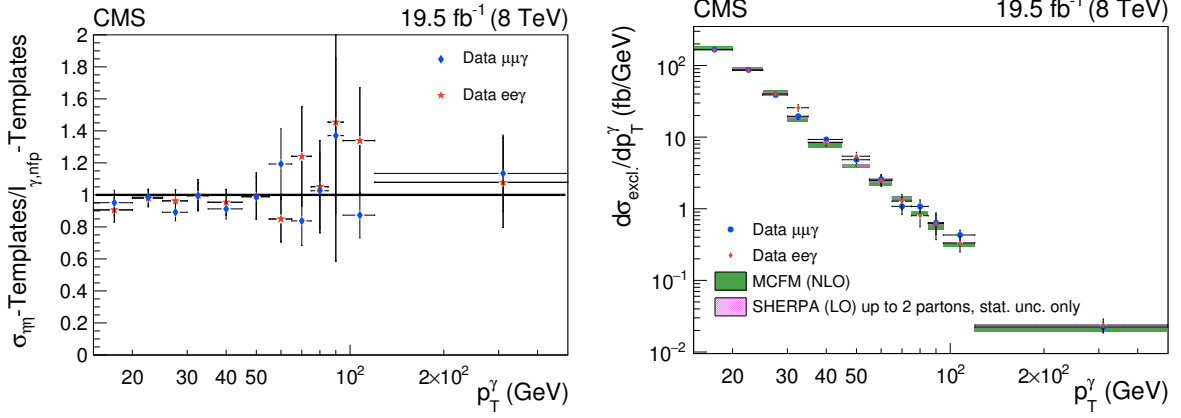


Figure 6: Left: ratio of the exclusive cross sections as obtained with the two template methods. Right: measured cross sections for the muon and electron channels using a combination of the two template methods compared to the MCFM (NLO) and the SHERPA SM predictions. The last bin is computed for the interval 120–500 GeV.

Table 3: The combined exclusive cross sections for muon and electron channels with statistical, systematic, and luminosity uncertainties respectively. Scale and PDF uncertainties are included in the systematics for the MCFM (NLO) cross section calculation.

p_T^γ (GeV)	σ_{excl} (fb)	$\sigma_{\text{excl}}^{\text{MCFM}}$ (fb)
15–20	$832 \pm 12 \pm 49 \pm 22$	873 ± 51
20–25	$432 \pm 9 \pm 25 \pm 11$	450 ± 23
25–30	$196 \pm 6 \pm 12 \pm 5$	211 ± 10
30–35	$100.5 \pm 5.3 \pm 7.4 \pm 2.6$	89.5 ± 7.9
35–45	$89.2 \pm 3.7 \pm 6.2 \pm 2.3$	77.2 ± 5.6
45–55	$49.5 \pm 2.8 \pm 4.9 \pm 1.3$	39.0 ± 2.4
55–65	$25.4 \pm 2.0 \pm 3.1 \pm 0.7$	22.4 ± 1.6
65–75	$11.4 \pm 1.5 \pm 1.7 \pm 0.3$	13.83 ± 0.98
75–85	$9.3 \pm 1.3 \pm 1.6 \pm 0.2$	8.85 ± 0.48
85–95	$6.3 \pm 1.2 \pm 1.4 \pm 0.2$	5.83 ± 0.70
95–120	$9.9 \pm 1.0 \pm 1.3 \pm 0.3$	7.83 ± 0.48
>120	$8.6 \pm 0.8 \pm 1.1 \pm 0.2$	7.81 ± 0.58

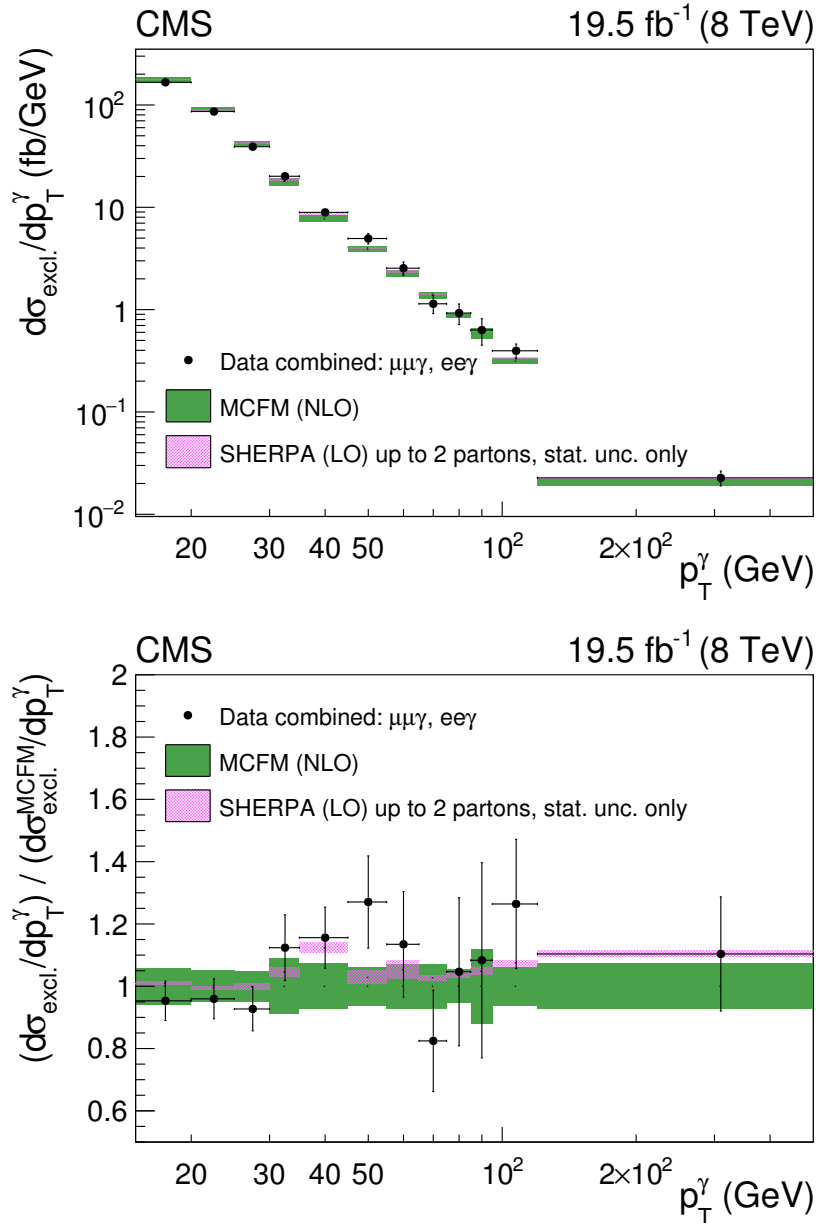


Figure 7: Top: combined exclusive differential cross section for the two lepton channels compared to the MCFM (NLO) and SHERPA SM predictions. The whole SHERPA sample (inclusive) is normalized to the NNLO cross section. The last bin is computed for the interval 120–500 GeV. Bottom: for the exclusive measurement the ratios to the MCFM (NLO) prediction are shown.

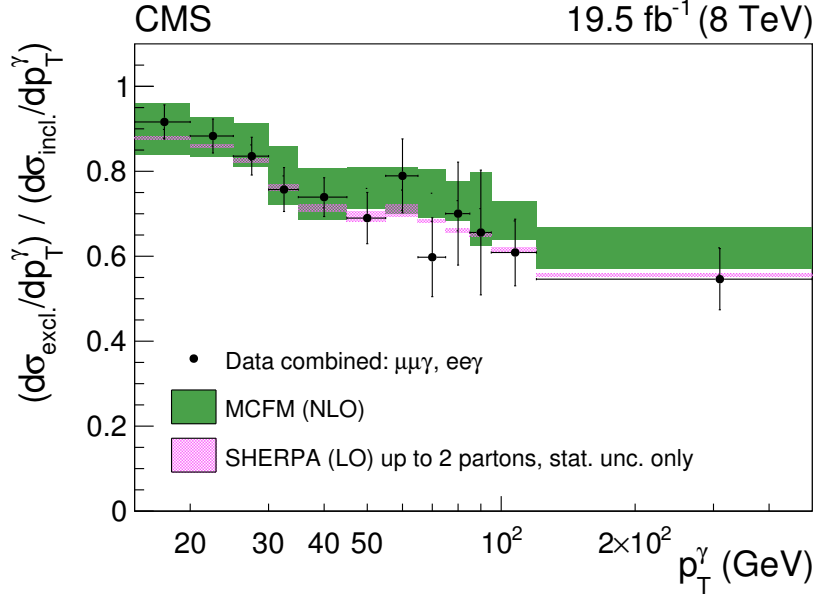


Figure 8: Ratio of the exclusive to inclusive cross sections for $Z\gamma$ production.

local $U(1)$ gauge symmetry. The resulting Lagrangian [35] has the form

$$\begin{aligned}
L_{\text{aTGC}} = L_{\text{SM}} + \frac{e}{m_Z^2} & \left[-[h_1^\gamma (\partial^\sigma F_{\sigma\mu}) + h_1^Z (\partial^\sigma Z_{\sigma\mu})] Z_\beta F^{\mu\beta} \right. \\
& - [h_3^\gamma (\partial_\sigma F^{\sigma\rho}) + h_3^Z (\partial_\sigma Z^{\sigma\rho})] Z^\alpha \tilde{F}_{\rho\alpha} \\
& - \left[\frac{h_2^\gamma}{m_Z^2} [\partial_\alpha \partial_\beta \partial^\rho F_{\rho\mu}] + \frac{h_2^Z}{m_Z^2} [\partial_\alpha \partial_\beta (\partial_\nu \partial^\nu + m_Z^2) Z_\mu] \right] Z^\alpha F^{\mu\beta} \\
& \left. + \left[\frac{h_4^\gamma}{2m_Z^2} [\partial_\nu \partial^\nu \partial^\sigma F^{\rho\alpha}] + \frac{h_4^Z}{2m_Z^2} [(\partial_\nu \partial^\nu + m_Z^2) \partial^\sigma Z^{\rho\alpha}] \right] Z_\sigma \tilde{F}_{\rho\alpha} \right] \quad (1)
\end{aligned}$$

with the electromagnetic tensor $F_{\mu\nu} = \partial_\mu F_\nu - \partial_\nu F_\mu$ and $\tilde{F}_{\mu\nu} = 1/2 \epsilon_{\mu\nu\rho\sigma} F^{\rho\sigma}$ and similar definitions for the Z boson field. There are eight coupling constants h_i^V , $i = 1 \dots 4$ and $V = Z, \gamma$ for $ZZ\gamma$ ($Z\gamma\gamma$) couplings. The parameters h_1^V and h_2^V are CP-violating while h_3^V and h_4^V are not. It was shown in Ref. [36, 37] that there is no dimension six operator respecting $U(1)_Y \times SU(2)_L$ invariance, but two dimension eight operators, including the Higgs field, that could lead to an enhancement proportional to h_1^V and h_3^V . In this measurement we follow the CMS convention of not using form factors [5].

For the $Z\gamma$ process the existence of aTGCs would typically lead to an enhancement of photons with high transverse momentum [1–3]. The observed p_T^γ distribution is therefore used to extract limits on $ZZ\gamma$ and $Z\gamma\gamma$ aTGCs.

The difference in the p_T^γ distributions between the SM and aTGCs models is parameterized using the MCFM (NLO) prediction. The NNLO SM calculation is added to describe a complete p_T^γ distributions of an aTGC model. To obtain a p_T^γ distribution that can be compared to the data, each simulated event is weighted by the lepton and photon efficiencies and the photon momentum is smeared according to the detector resolution. The irreducible background from the simulation and the background of nonprompt and misidentified photons, as obtained from the $\sigma_{\eta\eta}$ template method, are added. In order to obtain a smooth background description, the background is parameterized as a sum of two exponential functions with parameters

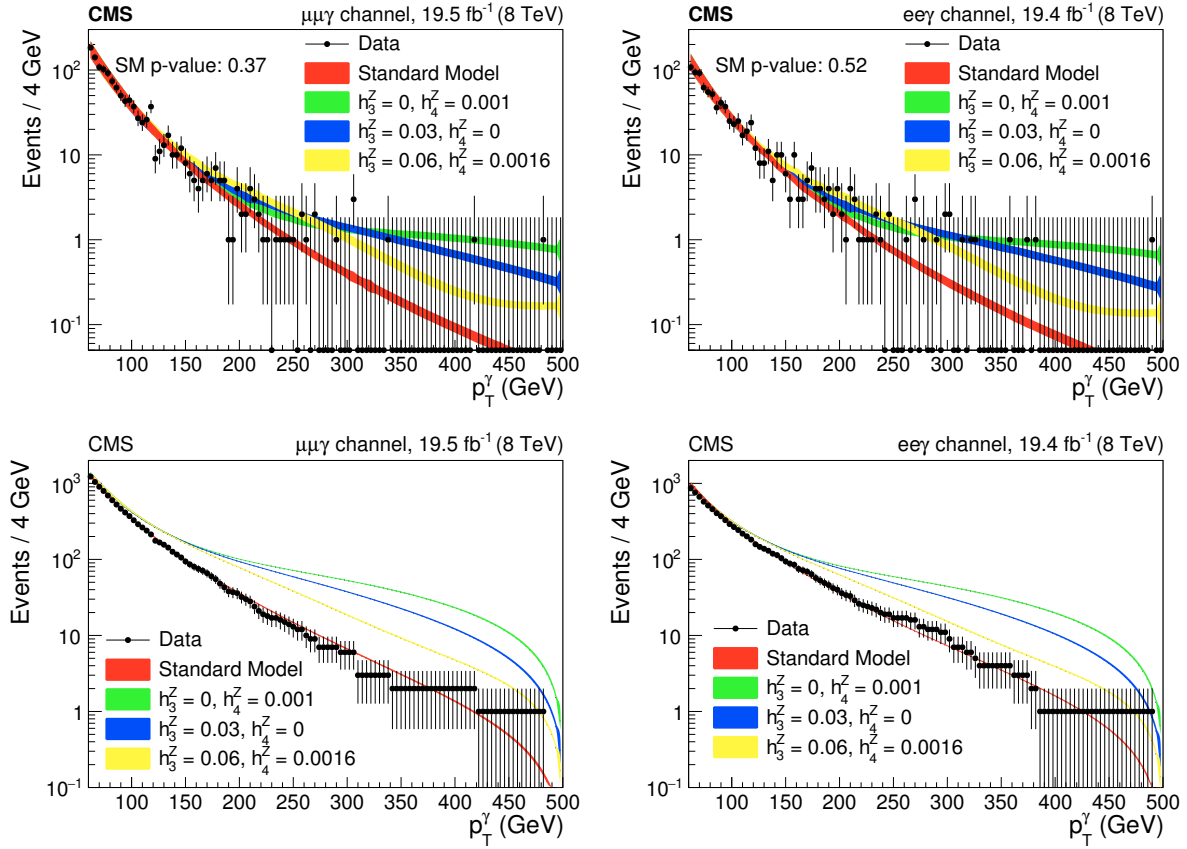


Figure 9: Top: the p_T^γ distribution compared to predictions using various values for the aTGCs and the SM. The observed p -values show that data are fully compatible with the SM expectation (red). Bottom: corresponding cumulated distributions.

obtained from a fit to the observed background distribution. Figure 9 shows a direct comparison between the p_T^γ distribution in data and the expectations for various aTGC strengths. A theoretical uncertainty of 6–12% is determined from PDF and scale variations. Experimental systematic uncertainties are 2% in the dilepton efficiency, 2% in the photon efficiency, 2.6% in the luminosity measurement, and depending on p_T^γ up to 8% uncertainty in the background of nonprompt and misidentified photons obtained from the $\sigma_{\eta\eta}$ template method.

An unbinned profile likelihood ratio based on the p_T^γ distribution is used to find the best fitting aTGC model and its 95% confidence level (CL) region. With the precision of the current measurement it is not possible to distinguish between the CP-even and CP-odd contributions. Therefore, only the CP-even parameters h_3^V and h_4^V are considered. The two-dimensional limits on h_3^V and h_4^V are shown in Fig. 10. The combination of the muon and electron channels takes into account that most of the systematic uncertainties are correlated with the exception of those related to the lepton reconstruction efficiencies. The one-dimensional 95% CL regions, when only one of the aTGCs is nonzero, are

$$\begin{aligned}
 -3.8 \times 10^{-3} &< h_3^Z < 3.7 \times 10^{-3} \\
 -3.1 \times 10^{-5} &< h_4^Z < 3.0 \times 10^{-5} \\
 -4.6 \times 10^{-3} &< h_3^\gamma < 4.6 \times 10^{-3} \\
 -3.6 \times 10^{-5} &< h_4^\gamma < 3.5 \times 10^{-5}.
 \end{aligned}$$

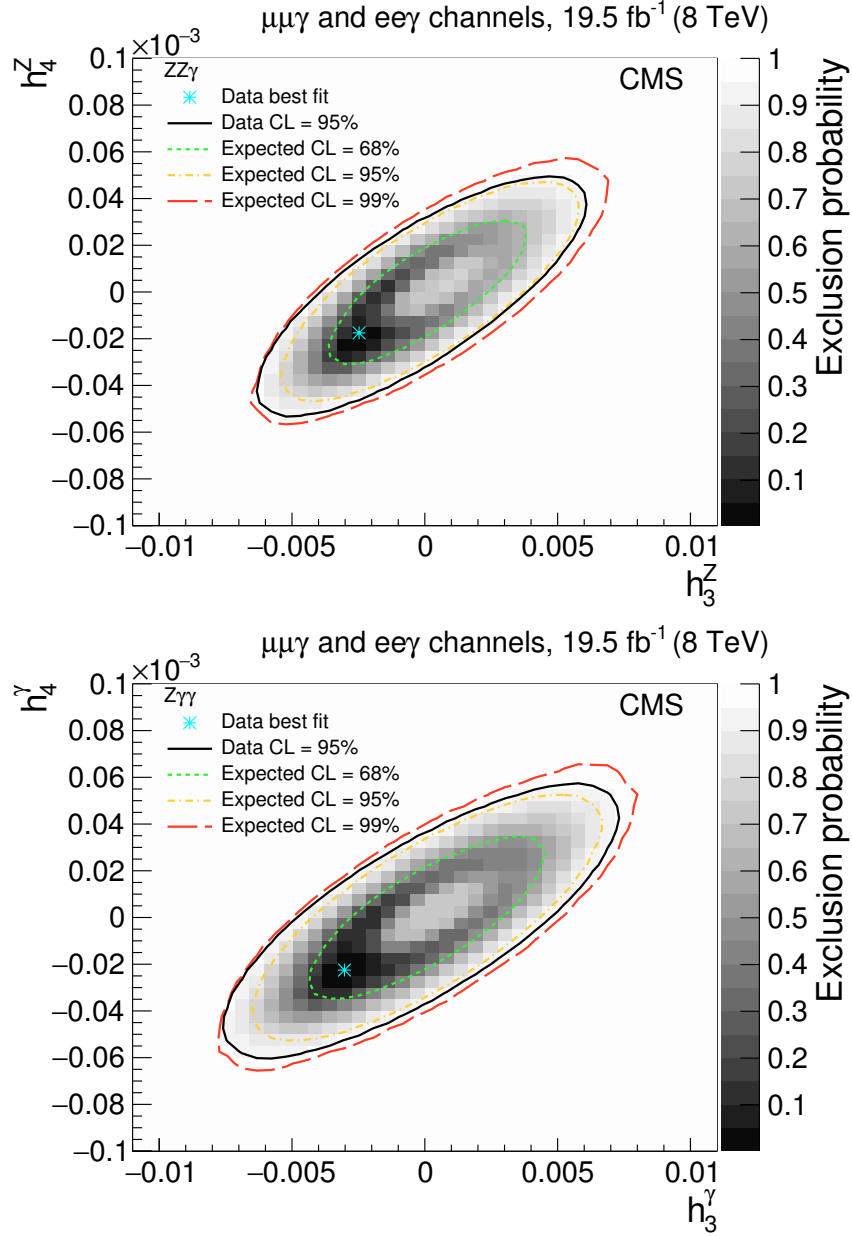


Figure 10: Best fit of the combined muon and electron channels for models of anomalous $ZZ\gamma$ (top) and $Z\gamma\gamma$ (bottom) couplings. No form factor is used. The light blue star indicates the point of highest probability. The level of gray represents the exclusion probability and the black line corresponds to the 95% CL limit. In addition, several expected contours from SM simulation are shown.

8 Summary

A study of $Z\gamma$ production in pp collisions at 8 TeV using data collected with the CMS experiment in 2012, corresponding to an integrated luminosity of 19.5 fb^{-1} was presented. Decays of the Z bosons into muons and electrons were used for the measurement of the differential $Z\gamma$ cross section as a function of p_T^γ for a phase space defined by the kinematic requirements on the final-state particles shown in Table 1. In addition, the exclusive differential $Z\gamma$ cross section for events with no accompanying central jets was presented. The inclusive and exclusive cross sections for $p_T^\gamma > 15 \text{ GeV}$ are measured to be:

$$\begin{aligned}\sigma_{\text{incl}} &= 2063 \pm 19 \text{ (stat)} \pm 98 \text{ (syst)} \pm 54 \text{ (lumi)} \text{ fb}, \\ \sigma_{\text{excl}} &= 1770 \pm 18 \text{ (stat)} \pm 115 \text{ (syst)} \pm 46 \text{ (lumi)} \text{ fb}.\end{aligned}$$

Both values are compatible with the SM expectations of $\sigma_{\text{incl}}^{\text{MCFM}} = 2100 \pm 120 \text{ fb}$ ($\sigma_{\text{incl}}^{\text{NNLO}} = 2241 \pm 22 \text{ fb}$) and $\sigma_{\text{excl}}^{\text{MCFM}} = 1800 \pm 120 \text{ fb}$, respectively. At high p_T^γ the inclusive measurement is well described by the NNLO calculation and also by the SHERPA prediction including up to two additional partons at matrix element level, while a clear excess is observed with respect to the MCFM (NLO) calculation. This emphasizes the importance of NNLO QCD corrections for this measurement. A similar excess is not observed for the exclusive measurement.

Limits on the strengths of anomalous $ZZ\gamma$ and $Z\gamma\gamma$ couplings have been extracted. The following one-dimensional limits at 95% CL have been obtained

$$\begin{aligned}-3.8 \times 10^{-3} &< h_3^Z < 3.7 \times 10^{-3} \\ -3.1 \times 10^{-5} &< h_4^Z < 3.0 \times 10^{-5} \\ -4.6 \times 10^{-3} &< h_3^\gamma < 4.6 \times 10^{-3} \\ -3.6 \times 10^{-5} &< h_4^\gamma < 3.5 \times 10^{-5}.\end{aligned}$$

These limits are more stringent than previously published results on neutral aTGCs for the charged lepton decays of the Z boson from LEP [38, 39], Tevatron [40, 41] and the LHC experiments [4, 5].

Acknowledgments

We thank Dirk Rathlev and Massimiliano Grazzini for providing us with the NNLO calculation of the cross section.

We congratulate our colleagues in the CERN accelerator departments for the excellent performance of the LHC and thank the technical and administrative staffs at CERN and at other CMS institutes for their contributions to the success of the CMS effort. In addition, we gratefully acknowledge the computing centers and personnel of the Worldwide LHC Computing Grid for delivering so effectively the computing infrastructure essential to our analyses. Finally, we acknowledge the enduring support for the construction and operation of the LHC and the CMS detector provided by the following funding agencies: the Austrian Federal Ministry of Science, Research and Economy and the Austrian Science Fund; the Belgian Fonds de la Recherche Scientifique, and Fonds voor Wetenschappelijk Onderzoek; the Brazilian Funding Agencies (CNPq, CAPES, FAPERJ, and FAPESP); the Bulgarian Ministry of Education and Science; CERN; the Chinese Academy of Sciences, Ministry of Science and Technology, and National Natural Science Foundation of China; the Colombian Funding Agency (COLCIENCIAS); the Croatian Ministry of Science, Education and Sport, and the Croatian Science Foundation;

the Research Promotion Foundation, Cyprus; the Ministry of Education and Research, Estonian Research Council via IUT23-4 and IUT23-6 and European Regional Development Fund, Estonia; the Academy of Finland, Finnish Ministry of Education and Culture, and Helsinki Institute of Physics; the Institut National de Physique Nucléaire et de Physique des Particules / CNRS, and Commissariat à l'Énergie Atomique et aux Énergies Alternatives / CEA, France; the Bundesministerium für Bildung und Forschung, Deutsche Forschungsgemeinschaft, and Helmholtz-Gemeinschaft Deutscher Forschungszentren, Germany; the General Secretariat for Research and Technology, Greece; the National Scientific Research Foundation, and National Innovation Office, Hungary; the Department of Atomic Energy and the Department of Science and Technology, India; the Institute for Studies in Theoretical Physics and Mathematics, Iran; the Science Foundation, Ireland; the Istituto Nazionale di Fisica Nucleare, Italy; the Ministry of Science, ICT and Future Planning, and National Research Foundation (NRF), Republic of Korea; the Lithuanian Academy of Sciences; the Ministry of Education, and University of Malaya (Malaysia); the Mexican Funding Agencies (CINVESTAV, CONACYT, SEP, and UASLP-FAI); the Ministry of Business, Innovation and Employment, New Zealand; the Pakistan Atomic Energy Commission; the Ministry of Science and Higher Education and the National Science Centre, Poland; the Fundação para a Ciência e a Tecnologia, Portugal; JINR, Dubna; the Ministry of Education and Science of the Russian Federation, the Federal Agency of Atomic Energy of the Russian Federation, Russian Academy of Sciences, and the Russian Foundation for Basic Research; the Ministry of Education, Science and Technological Development of Serbia; the Secretaría de Estado de Investigación, Desarrollo e Innovación and Programa Consolider-Ingenio 2010, Spain; the Swiss Funding Agencies (ETH Board, ETH Zurich, PSI, SNF, UniZH, Canton Zurich, and SER); the Ministry of Science and Technology, Taipei; the Thailand Center of Excellence in Physics, the Institute for the Promotion of Teaching Science and Technology of Thailand, Special Task Force for Activating Research and the National Science and Technology Development Agency of Thailand; the Scientific and Technical Research Council of Turkey, and Turkish Atomic Energy Authority; the National Academy of Sciences of Ukraine, and State Fund for Fundamental Researches, Ukraine; the Science and Technology Facilities Council, UK; the US Department of Energy, and the US National Science Foundation.

Individuals have received support from the Marie-Curie program and the European Research Council and EPLANET (European Union); the Leventis Foundation; the A. P. Sloan Foundation; the Alexander von Humboldt Foundation; the Belgian Federal Science Policy Office; the Fonds pour la Formation à la Recherche dans l'Industrie et dans l'Agriculture (FRIA-Belgium); the Agentschap voor Innovatie door Wetenschap en Technologie (IWT-Belgium); the Ministry of Education, Youth and Sports (MEYS) of the Czech Republic; the Council of Science and Industrial Research, India; the HOMING PLUS program of Foundation for Polish Science, cofinanced from European Union, Regional Development Fund; the Compagnia di San Paolo (Torino); the Consorzio per la Fisica (Trieste); MIUR project 20108T4XTM (Italy); the Thalís and Aristeia programs cofinanced by EU-ESF and the Greek NSRF; and the National Priorities Research Program by Qatar National Research Fund.

References

- [1] V. Barger, H. Baer, and K. Hagiwara, "Testing models for anomalous radiative decays of the Z boson", *Phys. Rev. D* **30** (1984) 1513, doi:10.1103/PhysRevD.30.1513.
- [2] U. Baur, T. Han, and J. Ohnemus, "QCD corrections and anomalous couplings in $Z\gamma$ production at hadron colliders", *Phys. Rev. D* **57** (1998) 2823, doi:10.1103/PhysRevD.57.2823, arXiv:hep-ph/9710416.

- [3] U. Baur and E. L. Berger, “Probing the weak-boson sector in $Z\gamma$ production at hadron colliders”, *Phys. Rev. D* (1993) 4889, doi:10.1103/PhysRevD.47.4889.
- [4] ATLAS Collaboration, “Measurements of $W\gamma$ and $Z\gamma$ production in pp collisions at $\sqrt{s} = 7$ TeV with the ATLAS detector at the LHC”, *Phys. Rev. D* **87** (2013) 112003, doi:10.1103/PhysRevD.87.112003, arXiv:1302.1283.
- [5] CMS Collaboration, “Measurement of the $W\gamma$ and $Z\gamma$ inclusive cross sections in pp collisions at $\sqrt{s} = 7$ TeV and limits on anomalous triple gauge boson couplings”, *Phys. Rev. D* **89** (2014) 092005, doi:10.1103/PhysRevD.89.092005.
- [6] CMS Collaboration, “Particle-Flow Event Reconstruction in CMS and Performance for Jets, Taus, and E_T^{miss} ”, CMS Physics Analysis Summary CMS-PAS-PFT-09-001, 2009.
- [7] CMS Collaboration, “Commissioning of the particle-flow event reconstruction with the first LHC collisions recorded in the CMS detector”, CMS Physics Analysis Summary CMS-PAS-PFT-10-001, 2010.
- [8] CMS Collaboration, “Commissioning of the particle-flow event reconstruction with leptons from J/Ψ and W decays at 7 TeV”, CMS Physics Analysis Summary CMS-PAS-PFT-10-003, 2010.
- [9] W. Adam, R. Frühwirth, A. Strandlie, and T. Todorov, “Reconstruction of electrons with the Gaussian-sum filter in the CMS tracker at the LHC”, *J. Phys. G: Nucl. Part. Phys.* **31** (2005) N9, doi:10.1088/0954-3899/31/9/N01.
- [10] S. Baffioni et al., “Electron reconstruction in CMS”, *Eur. Phys. J. C* **49** (2007) 1099, doi:10.1140/epjc/s10052-006-0175-5.
- [11] M. Cacciari, G. P. Salam, and G. Soyez, “The anti- k_t jet clustering algorithm”, *JHEP* **04** (2008) 063, doi:10.1088/1126-6708/2008/04/063, arXiv:0802.1189.
- [12] M. Cacciari, G. P. Salam, and G. Soyez, “FastJet user manual”, *Eur. Phys. J. C* **72** (2012) 1896, doi:10.1140/epjc/s10052-012-1896-2, arXiv:1111.6097.
- [13] CMS Collaboration, “Determination of jet energy calibration and transverse momentum resolution in CMS”, *J. Instrum.* **6** (2011) P11002, doi:10.1088/1748-0221/6/11/P11002.
- [14] M. Cacciari, G. P. Salam, and G. Soyez, “The catchment area of jets”, *JHEP* **04** (2008) 005, doi:10.1088/1126-6708/2008/04/005, arXiv:0802.1188.
- [15] CMS Collaboration, “The CMS experiment at the CERN LHC”, *JINST* **3** (2008) S08004, doi:10.1088/1748-0221/3/08/S08004.
- [16] T. Gleisberg et al., “Event generation with SHERPA 1.1”, *JHEP* **02** (2009) 007, doi:10.1088/1126-6708/2009/02/007, arXiv:0811.4622.
- [17] J. M. Campbell, H. B. Hartanto, and C. Williams, “Next-to-leading order predictions for $Z\gamma$ +jet and $Z\gamma\gamma$ final states at the LHC”, *JHEP* **11** (2012) 162, doi:10.1007/JHEP11(2012)162, arXiv:1208.0566.
- [18] H.-L. Lai et al., “New parton distributions for collider physics”, *Phys. Rev. D* **82** (2010) 074024, doi:10.1103/PhysRevD.82.074024, arXiv:1007.2241.

- [19] J. M. Campbell, W. Huston, J. and W. J. Stirling, “Hard interactions of quarks and gluons: a primer for LHC physics”, *Rep. Prog. Phys.* **70** (2007) 89, doi:10.1088/0034-4885/70/1/R02, arXiv:hep-ph/0611148.
- [20] I. W. Stewart and F. J. Tackmann, “Theory uncertainties for Higgs mass and other searches using jet bins”, *Phys. Rev. D* **85** (2012) 034011, doi:10.1103/PhysRevD.85.034011, arXiv:1107.2117.
- [21] M. Grazzini, S. Kallweit, D. Rathlev, and A. Torre, “ $Z\gamma$ production at hadron colliders in NNLO QCD”, *Phys. Lett. B* **731** (2014) 204, doi:10.1016/j.physletb.2014.02.037, arXiv:1309.7000.
- [22] J. Alwall et al., “MadGraph/MadEvent v4: the new web generation”, *JHEP* **09** (2007) 028, doi:10.1088/1126-6708/2007/09/028, arXiv:0706.2334.
- [23] J. Pumplin et al., “New generation of parton distributions with uncertainties from global QCD analysis”, *JHEP* **07** (2002) 012, doi:10.1088/1126-6708/2002/07/012, arXiv:hep-ph/0201195.
- [24] T. Sjöstrand, S. Mrenna, and P. Skands, “PYTHIA 6.4 physics and manual”, *JHEP* **05** (2006) 026, doi:10.1088/1126-6708/2006/05/026, arXiv:hep-ph/0603175.
- [25] R. Gavin, Y. Li, F. Petriello, and S. Quackenbush, “FEWZ 2.0: A code for hadronic Z production at next-to-next-to-leading order”, *Comp. Phys. Comm.* **182** (2011) 2388, doi:10.1016/j.cpc.2011.06.008.
- [26] GEANT4 Collaboration, “GEANT4—a simulation toolkit”, *Nucl. Instrum. Meth. A* **506** (2003) 250, doi:10.1016/S0168-9002(03)01368-8.
- [27] CMS Collaboration, “Performance of CMS muon reconstruction in pp collision events at $\sqrt{s} = 7$ TeV”, *J. Instrum.* **7** (2012) P10002, doi:10.1088/1748-0221/7/10/P10002.
- [28] CMS Collaboration, “Electron performance with 19.6 fb^{-1} of data collected at $\sqrt{s} = 8$ TeV with the CMS detector.”, CMS Detector Performance Summary CMS-DP-2013-003, 2013.
- [29] M. Cacciari and G. P. Salam, “Pileup subtraction using jet areas”, *Phys. Lett. B* **659** (2008) 119, doi:10.1016/j.physletb.2007.09.077, arXiv:0707.1378.
- [30] CMS Collaboration, “Measurement of the isolated prompt diphoton production cross section in pp collisions at $\sqrt{s}=7$ TeV”, *J. High Energy Phys.* **01** (2012) 133, doi:10.1007/JHEP01(2012)133.
- [31] CMS Collaboration, “Measurement of the inclusive W and Z production cross sections in pp collisions at $\sqrt{s} = 7$ TeV with the CMS experiment”, *J. High Energy Phys.* **10** (2011) 132, doi:10.1007/JHEP10(2011)132.
- [32] G. D’Agostini, “A multidimensional unfolding method based on Bayes’ theorem”, *Nucl. Instrum. Meth. A* **362** (1995) 487, doi:10.1016/0168-9002(95)00274-X.
- [33] T. Auye, “Unfolding algorithms and tests using RooUnfold”, (2011). arXiv:1105.1160.
- [34] A. Valassi, “Combining correlated measurements of several different physical quantities”, *Nucl. Instrum. Meth. A* **500** (2003) 391, doi:10.1016/S0168-9002(03)00329-2.

- [35] G. J. Gounaris, J. Layssac, and F. M. Renard, "Signatures of the anomalous $Z\gamma$ and ZZ production at lepton and hadron colliders", *Phys. Rev. D* **61** (2000) 3013, doi:10.1103/PhysRevD.61.073013, arXiv:hep-ph/9910395.
- [36] G. J. Gounaris, J. Layssac, and F. M. Renard, "Off-shell structure of the anomalous Z and γ self-couplings", *Phys. Rev. D* **62** (2000) 073012, doi:10.1103/PhysRevD.62.073012.
- [37] C. Degrande, "A basis of dimension-eight operators for anomalous neutral triple gauge boson interactions", *JHEP* **02** (2014) 101, doi:10.1007/JHEP02(2014)101, arXiv:1308.6323.
- [38] L3 Collaboration, "Study of the $e^+e^- \rightarrow Z\gamma$ process at LEP and limits on triple neutral-gauge-boson couplings", *Phys. Lett. B* **597** (2004) 119, doi:10.1016/j.physletb.2004.07.002.
- [39] OPAL Collaboration, "Study of Z pair production and anomalous couplings in e^+e^- collisions at \sqrt{s} between 190 GeV and 209 GeV", *Eur. Phys. J. C* **32** (2003) 303, doi:10.1140/epjc/s2003-01467-x, arXiv:hep-ex/0310013.
- [40] CDF Collaboration, "Limits on Anomalous Trilinear Gauge Couplings in $Z\gamma$ Events from $p\bar{p}$ Collisions at $\sqrt{s} = 1.96$ TeV", *Phys. Rev. Lett.* **107** (2011) 051802, doi:10.1103/PhysRevLett.107.051802.
- [41] D0 Collaboration, " $Z\gamma$ production and limits on anomalous $ZZ\gamma$ and $Z\gamma\gamma$ couplings in $p\bar{p}$ collisions at $\sqrt{s} = 1.96$ TeV", *Phys. Rev. D* **85** (2012) 052001, doi:10.1103/PhysRevD.85.052001, arXiv:1111.3684.

A The CMS Collaboration

Yerevan Physics Institute, Yerevan, Armenia

V. Khachatryan, A.M. Sirunyan, A. Tumasyan

Institut für Hochenergiephysik der OeAW, Wien, Austria

W. Adam, T. Bergauer, M. Dragicevic, J. Erö, M. Friedl, R. Frühwirth¹, V.M. Ghete, C. Hartl, N. Hörmann, J. Hrubec, M. Jeitler¹, W. Kiesenhofer, V. Knünz, M. Krammer¹, I. Krätschmer, D. Liko, I. Mikulec, D. Rabadý², B. Rahbaran, H. Rohringer, R. Schöfbeck, J. Strauss, W. Treberer-Treberspurg, W. Waltenberger, C.-E. Wulz¹

National Centre for Particle and High Energy Physics, Minsk, Belarus

V. Mossolov, N. Shumeiko, J. Suarez Gonzalez

Universiteit Antwerpen, Antwerpen, Belgium

S. Alderweireldt, S. Bansal, T. Cornelis, E.A. De Wolf, X. Janssen, A. Knutsson, J. Lauwers, S. Luyckx, S. Ochesanu, R. Rougny, M. Van De Klundert, H. Van Haeevermaet, P. Van Mechelen, N. Van Remortel, A. Van Spilbeeck

Vrije Universiteit Brussel, Brussel, Belgium

F. Blekman, S. Blyweert, J. D'Hondt, N. Daci, N. Heracleous, J. Keaveney, S. Lowette, M. Maes, A. Olbrechts, Q. Python, D. Strom, S. Tavernier, W. Van Doninck, P. Van Mulders, G.P. Van Onsem, I. Vilella

Université Libre de Bruxelles, Bruxelles, Belgium

C. Caillol, B. Clerbaux, G. De Lentdecker, D. Dobur, L. Favart, A.P.R. Gay, A. Grebenyuk, A. Léonard, A. Mohammadi, L. Pernie², A. Randle-conde, T. Reis, T. Seva, L. Thomas, C. Vander Velde, P. Vanlaer, J. Wang, F. Zenoni

Ghent University, Ghent, Belgium

V. Adler, K. Beernaert, L. Benucci, A. Cimmino, S. Costantini, S. Crucy, S. Dildick, A. Fagot, G. Garcia, J. Mccartin, A.A. Ocampo Rios, D. Poyraz, D. Ryckbosch, S. Salva Diblen, M. Sigamani, N. Strobbe, F. Thyssen, M. Tytgat, E. Yazgan, N. Zaganidis

Université Catholique de Louvain, Louvain-la-Neuve, Belgium

S. Basegmez, C. Beluffi³, G. Bruno, R. Castello, A. Caudron, L. Ceard, G.G. Da Silveira, C. Delaere, T. du Pree, D. Favart, L. Forthomme, A. Giammanco⁴, J. Hollar, A. Jafari, P. Jez, M. Komm, V. Lemaitre, C. Nuttens, L. Perrini, A. Pin, K. Piotrkowski, A. Popov⁵, L. Quertenmont, M. Selvaggi, M. Vidal Marono, J.M. Vizan Garcia

Université de Mons, Mons, Belgium

N. Bely, T. Caebegs, E. Daubie, G.H. Hammad

Centro Brasileiro de Pesquisas Fisicas, Rio de Janeiro, Brazil

W.L. Aldá Júnior, G.A. Alves, L. Brito, M. Correa Martins Junior, T. Dos Reis Martins, J. Molina, C. Mora Herrera, M.E. Pol, P. Rebello Teles

Universidade do Estado do Rio de Janeiro, Rio de Janeiro, Brazil

W. Carvalho, J. Chinellato⁶, A. Custódio, E.M. Da Costa, D. De Jesus Damiao, C. De Oliveira Martins, S. Fonseca De Souza, H. Malbouisson, D. Matos Figueiredo, L. Mundim, H. Nogima, W.L. Prado Da Silva, J. Santaolalla, A. Santoro, A. Sznajder, E.J. Tonelli Manganote⁶, A. Vilela Pereira

Universidade Estadual Paulista ^a, Universidade Federal do ABC ^b, São Paulo, Brazil

C.A. Bernardes^b, S. Dogra^a, T.R. Fernandez Perez Tomei^a, E.M. Gregores^b, P.G. Mercadante^b, S.F. Novaes^a, Sandra S. Padula^a

Institute for Nuclear Research and Nuclear Energy, Sofia, Bulgaria

A. Aleksandrov, V. Genchev², R. Hadjiiska, P. Iaydjiev, A. Marinov, S. Piperov, M. Rodozov, S. Stoykova, G. Sultanov, M. Vutova

University of Sofia, Sofia, Bulgaria

A. Dimitrov, I. Glushkov, L. Litov, B. Pavlov, P. Petkov

Institute of High Energy Physics, Beijing, China

J.G. Bian, G.M. Chen, H.S. Chen, M. Chen, T. Cheng, R. Du, C.H. Jiang, R. Plestina⁷, F. Romeo, J. Tao, Z. Wang

State Key Laboratory of Nuclear Physics and Technology, Peking University, Beijing, China

C. Asawatangtrakuldee, Y. Ban, Q. Li, S. Liu, Y. Mao, S.J. Qian, D. Wang, Z. Xu, W. Zou

Universidad de Los Andes, Bogota, Colombia

C. Avila, A. Cabrera, L.F. Chaparro Sierra, C. Florez, J.P. Gomez, B. Gomez Moreno, J.C. Sanabria

University of Split, Faculty of Electrical Engineering, Mechanical Engineering and Naval Architecture, Split, Croatia

N. Godinovic, D. Lelas, D. Polic, I. Puljak

University of Split, Faculty of Science, Split, Croatia

Z. Antunovic, M. Kovac

Institute Rudjer Boskovic, Zagreb, Croatia

V. Brigljevic, K. Kadija, J. Luetic, D. Mekterovic, L. Sudic

University of Cyprus, Nicosia, Cyprus

A. Attikis, G. Mavromanolakis, J. Mousa, C. Nicolaou, F. Ptochos, P.A. Razis

Charles University, Prague, Czech Republic

M. Bodlak, M. Finger, M. Finger Jr.⁸

Academy of Scientific Research and Technology of the Arab Republic of Egypt, Egyptian Network of High Energy Physics, Cairo, Egypt

Y. Assran⁹, A. Ellithi Kamel¹⁰, M.A. Mahmoud¹¹, A. Radi^{12,13}

National Institute of Chemical Physics and Biophysics, Tallinn, Estonia

M. Kadastik, M. Murumaa, M. Raidal, A. Tiko

Department of Physics, University of Helsinki, Helsinki, Finland

P. Eerola, M. Voutilainen

Helsinki Institute of Physics, Helsinki, Finland

J. Härkönen, V. Karimäki, R. Kinnunen, M.J. Kortelainen, T. Lampén, K. Lassila-Perini, S. Lehti, T. Lindén, P. Luukka, T. Mäenpää, T. Peltola, E. Tuominen, J. Tuominiemi, E. Tuovinen, L. Wendland

Lappeenranta University of Technology, Lappeenranta, Finland

J. Talvitie, T. Tuuva

DSM/IRFU, CEA/Saclay, Gif-sur-Yvette, France

M. Besancon, F. Couderc, M. Dejardin, D. Denegri, B. Fabbro, J.L. Faure, C. Favaro, F. Ferri, S. Ganjour, A. Givernaud, P. Gras, G. Hamel de Monchenault, P. Jarry, E. Locci, J. Malcles, J. Rander, A. Rosowsky, M. Titov

Laboratoire Leprince-Ringuet, Ecole Polytechnique, IN2P3-CNRS, Palaiseau, France

S. Baffioni, F. Beaudette, P. Busson, E. Chapon, C. Charlot, T. Dahms, M. Dalchenko, L. Dobrzynski, N. Filipovic, A. Florent, R. Granier de Cassagnac, L. Mastrolorenzo, P. Miné, I.N. Naranjo, M. Nguyen, C. Ochando, G. Ortona, P. Paganini, S. Regnard, R. Salerno, J.B. Sauvan, Y. Sirois, C. Veelken, Y. Yilmaz, A. Zabi

Institut Pluridisciplinaire Hubert Curien, Université de Strasbourg, Université de Haute Alsace Mulhouse, CNRS/IN2P3, Strasbourg, France

J.-L. Agram¹⁴, J. Andrea, A. Aubin, D. Bloch, J.-M. Brom, E.C. Chabert, C. Collard, E. Conte¹⁴, J.-C. Fontaine¹⁴, D. Gelé, U. Goerlach, C. Goetzmann, A.-C. Le Bihan, K. Skovpen, P. Van Hove

Centre de Calcul de l'Institut National de Physique Nucleaire et de Physique des Particules, CNRS/IN2P3, Villeurbanne, France

S. Gadrat

Université de Lyon, Université Claude Bernard Lyon 1, CNRS-IN2P3, Institut de Physique Nucléaire de Lyon, Villeurbanne, France

S. Beauceron, N. Beaupere, C. Bernet⁷, G. Boudoul², E. Bouvier, S. Brochet, C.A. Carrillo Montoya, J. Chasserat, R. Chierici, D. Contardo², P. Depasse, H. El Mamouni, J. Fan, J. Fay, S. Gascon, M. Gouzevitch, B. Ille, T. Kurca, M. Lethuillier, L. Mirabito, S. Perries, J.D. Ruiz Alvarez, D. Sabes, L. Sgandurra, V. Sordini, M. Vander Donckt, P. Verdier, S. Viret, H. Xiao

Institute of High Energy Physics and Informatization, Tbilisi State University, Tbilisi, Georgia

Z. Tsamalaidze⁸

RWTH Aachen University, I. Physikalisches Institut, Aachen, Germany

C. Autermann, S. Beranek, M. Bontenackels, M. Edelhoff, L. Feld, A. Heister, K. Klein, M. Lipinski, A. Ostapchuk, M. Preuten, F. Raupach, J. Sammet, S. Schael, J.F. Schulte, H. Weber, B. Wittmer, V. Zhukov⁵

RWTH Aachen University, III. Physikalisches Institut A, Aachen, Germany

M. Ata, M. Brodski, E. Dietz-Laursonn, D. Duchardt, M. Erdmann, R. Fischer, A. Güth, T. Hebbeker, C. Heidemann, K. Hoepfner, D. Klingebiel, S. Knutzen, P. Kreuzer, M. Merschmeyer, A. Meyer, P. Millet, M. Olschewski, K. Padeken, P. Papacz, H. Reithler, S.A. Schmitz, L. Sonnenschein, D. Teyssier, S. Thüer, M. Weber

RWTH Aachen University, III. Physikalisches Institut B, Aachen, Germany

V. Cherepanov, Y. Erdogan, G. Flügge, H. Geenen, M. Geisler, W. Haj Ahmad, F. Hoehle, B. Kargoll, T. Kress, Y. Kuessel, A. Künsken, J. Lingemann², A. Nowack, I.M. Nugent, O. Pooth, A. Stahl

Deutsches Elektronen-Synchrotron, Hamburg, Germany

M. Aldaya Martin, I. Asin, N. Bartosik, J. Behr, U. Behrens, A.J. Bell, A. Bethani, K. Borras, A. Burgmeier, A. Cakir, L. Calligaris, A. Campbell, S. Choudhury, F. Costanza, C. Diez Pardos, G. Dolinska, S. Dooling, T. Dorland, G. Eckerlin, D. Eckstein, T. Eichhorn, G. Flucke, J. Garay Garcia, A. Geiser, P. Gunnellini, J. Hauk, M. Hempel¹⁵, H. Jung, A. Kalogeropoulos, M. Kasemann, P. Katsas, J. Kieseler, C. Kleinwort, I. Korol, D. Krücker, W. Lange, J. Leonard, K. Lipka, A. Lobanov, W. Lohmann¹⁵, B. Lutz, R. Mankel, I. Marfin¹⁵, I.-A. Melzer-Pellmann,

A.B. Meyer, G. Mittag, J. Mnich, A. Mussgiller, S. Naumann-Emme, A. Nayak, E. Ntomari, H. Perrey, D. Pitzl, R. Placakyte, A. Raspereza, P.M. Ribeiro Cipriano, B. Roland, E. Ron, M.Ö. Sahin, J. Salfeld-Nebgen, P. Saxena, T. Schoerner-Sadenius, M. Schröder, C. Seitz, S. Spannagel, A.D.R. Vargas Trevino, R. Walsh, C. Wissing

University of Hamburg, Hamburg, Germany

V. Blobel, M. Centis Vignali, A.R. Draeger, J. Erfle, E. Garutti, K. Goebel, M. Görner, J. Haller, M. Hoffmann, R.S. Höing, A. Junkes, H. Kirschenmann, R. Klanner, R. Kogler, J. Lange, T. Lapsien, T. Lenz, I. Marchesini, J. Ott, T. Peiffer, A. Perieanu, N. Pietsch, J. Poehlsen, T. Poehlsen, D. Rathjens, C. Sander, H. Schettler, P. Schleper, E. Schlieckau, A. Schmidt, M. Seidel, V. Sola, H. Stadie, G. Steinbrück, D. Troendle, E. Usai, L. Vanelderen, A. Vanhoefer

Institut für Experimentelle Kernphysik, Karlsruhe, Germany

C. Barth, C. Baus, J. Berger, C. Böser, E. Butz, T. Chwalek, W. De Boer, A. Descroix, A. Dierlamm, M. Feindt, F. Frensch, M. Giffels, A. Gilbert, F. Hartmann², T. Hauth, U. Husemann, I. Katkov⁵, A. Kornmayer², P. Lobelle Pardo, M.U. Mozer, T. Müller, Th. Müller, A. Nürnberg, G. Quast, K. Rabbertz, S. Röcker, H.J. Simonis, F.M. Stober, R. Ulrich, J. Wagner-Kuhr, S. Wayand, T. Weiler, R. Wolf

Institute of Nuclear and Particle Physics (INPP), NCSR Demokritos, Aghia Paraskevi, Greece

G. Anagnostou, G. Daskalakis, T. Gerasis, V.A. Giakoumopoulou, A. Kyriakis, D. Loukas, A. Markou, C. Markou, A. Psallidas, I. Topsis-Giotis

University of Athens, Athens, Greece

A. Agapitos, S. Kesisoglou, A. Panagiotou, N. Saoulidou, E. Stiliaris

University of Ioánnina, Ioánnina, Greece

X. Aslanoglou, I. Evangelou, G. Flouris, C. Foudas, P. Kokkas, N. Manthos, I. Papadopoulos, E. Paradas, J. Strogas

Wigner Research Centre for Physics, Budapest, Hungary

G. Bencze, C. Hajdu, P. Hidas, D. Horvath¹⁶, F. Sikler, V. Veszpremi, G. Vesztergombi¹⁷, A.J. Zsigmond

Institute of Nuclear Research ATOMKI, Debrecen, Hungary

N. Beni, S. Czellar, J. Karancsi¹⁸, J. Molnar, J. Palinkas, Z. Szillasi

University of Debrecen, Debrecen, Hungary

A. Makovec, P. Raics, Z.L. Trocsanyi, B. Ujvari

National Institute of Science Education and Research, Bhubaneswar, India

S.K. Swain

Panjab University, Chandigarh, India

S.B. Beri, V. Bhatnagar, R. Gupta, U. Bhawandeep, A.K. Kalsi, M. Kaur, R. Kumar, M. Mittal, N. Nishu, J.B. Singh

University of Delhi, Delhi, India

Ashok Kumar, Arun Kumar, S. Ahuja, A. Bhardwaj, B.C. Choudhary, A. Kumar, S. Malhotra, M. Naimuddin, K. Ranjan, V. Sharma

Saha Institute of Nuclear Physics, Kolkata, India

S. Banerjee, S. Bhattacharya, K. Chatterjee, S. Dutta, B. Gomber, Sa. Jain, Sh. Jain, R. Khurana, A. Modak, S. Mukherjee, D. Roy, S. Sarkar, M. Sharan

Bhabha Atomic Research Centre, Mumbai, India

A. Abdulsalam, D. Dutta, V. Kumar, A.K. Mohanty², L.M. Pant, P. Shukla, A. Topkar

Tata Institute of Fundamental Research, Mumbai, India

T. Aziz, S. Banerjee, S. Bhowmik¹⁹, R.M. Chatterjee, R.K. Dewanjee, S. Dugad, S. Ganguly, S. Ghosh, M. Guchait, A. Gurtu²⁰, G. Kole, S. Kumar, M. Maity¹⁹, G. Majumder, K. Mazumdar, G.B. Mohanty, B. Parida, K. Sudhakar, N. Wickramage²¹

Institute for Research in Fundamental Sciences (IPM), Tehran, Iran

H. Bakhshiansohi, H. Behnamian, S.M. Etesami²², A. Fahim²³, R. Goldouzian, M. Khakzad, M. Mohammadi Najafabadi, M. Naseri, S. Paktinat Mehdiabadi, F. Rezaei Hosseinabadi, B. Safarzadeh²⁴, M. Zeinali

University College Dublin, Dublin, Ireland

M. Felcini, M. Grunewald

INFN Sezione di Bari ^a, Università di Bari ^b, Politecnico di Bari ^c, Bari, Italy

M. Abbrescia^{a,b}, C. Calabria^{a,b}, S.S. Chhibra^{a,b}, A. Colaleo^a, D. Creanza^{a,c}, N. De Filippis^{a,c}, M. De Palma^{a,b}, L. Fiore^a, G. Iaselli^{a,c}, G. Maggi^{a,c}, M. Maggi^a, S. My^{a,c}, S. Nuzzo^{a,b}, A. Pompili^{a,b}, G. Pugliese^{a,c}, R. Radogna^{a,b,2}, G. Selvaggi^{a,b}, A. Sharma^a, L. Silvestris^{a,2}, R. Venditti^{a,b}, P. Verwilligen^a

INFN Sezione di Bologna ^a, Università di Bologna ^b, Bologna, Italy

G. Abbiendi^a, A.C. Benvenuti^a, D. Bonacorsi^{a,b}, S. Braibant-Giacomelli^{a,b}, L. Brigliadori^{a,b}, R. Campanini^{a,b}, P. Capiluppi^{a,b}, A. Castro^{a,b}, F.R. Cavallo^a, G. Codispoti^{a,b}, M. Cuffiani^{a,b}, G.M. Dallavalle^a, F. Fabbri^a, A. Fanfani^{a,b}, D. Fasanella^{a,b}, P. Giacomelli^a, C. Grandi^a, L. Guiducci^{a,b}, S. Marcellini^a, G. Masetti^a, A. Montanari^a, F.L. Navarria^{a,b}, A. Perrotta^a, F. Primavera^{a,b}, A.M. Rossi^{a,b}, T. Rovelli^{a,b}, G.P. Siroli^{a,b}, N. Tosi^{a,b}, R. Travaglini^{a,b}

INFN Sezione di Catania ^a, Università di Catania ^b, CSFNSM ^c, Catania, Italy

S. Albergo^{a,b}, G. Cappello^a, M. Chiorboli^{a,b}, S. Costa^{a,b}, F. Giordano^{a,2}, R. Potenza^{a,b}, A. Tricomi^{a,b}, C. Tuve^{a,b}

INFN Sezione di Firenze ^a, Università di Firenze ^b, Firenze, Italy

G. Barbagli^a, V. Ciulli^{a,b}, C. Civinini^a, R. D'Alessandro^{a,b}, E. Focardi^{a,b}, E. Gallo^a, S. Gonzi^{a,b}, V. Gori^{a,b}, P. Lenzi^{a,b}, M. Meschini^a, S. Paoletti^a, G. Sguazzoni^a, A. Tropiano^{a,b}

INFN Laboratori Nazionali di Frascati, Frascati, Italy

L. Benussi, S. Bianco, F. Fabbri, D. Piccolo

INFN Sezione di Genova ^a, Università di Genova ^b, Genova, Italy

R. Ferretti^{a,b}, F. Ferro^a, M. Lo Vetere^{a,b}, E. Robutti^a, S. Tosi^{a,b}

INFN Sezione di Milano-Bicocca ^a, Università di Milano-Bicocca ^b, Milano, Italy

M.E. Dinardo^{a,b}, S. Fiorendi^{a,b}, S. Gennai^{a,2}, R. Gerosa^{a,b,2}, A. Ghezzi^{a,b}, P. Govoni^{a,b}, M.T. Lucchini^{a,b,2}, S. Malvezzi^a, R.A. Manzoni^{a,b}, A. Martelli^{a,b}, B. Marzocchi^{a,b,2}, D. Menasce^a, L. Moroni^a, M. Paganoni^{a,b}, D. Pedrini^a, S. Ragazzi^{a,b}, N. Redaelli^a, T. Tabarelli de Fatis^{a,b}

INFN Sezione di Napoli ^a, Università di Napoli 'Federico II' ^b, Università della Basilicata (Potenza) ^c, Università G. Marconi (Roma) ^d, Napoli, Italy

S. Buontempo^a, N. Cavallo^{a,c}, S. Di Guida^{a,d,2}, F. Fabozzi^{a,c}, A.O.M. Iorio^{a,b}, L. Lista^a, S. Meola^{a,d,2}, M. Merola^a, P. Paolucci^{a,2}

INFN Sezione di Padova ^a, Università di Padova ^b, Università di Trento (Trento) ^c, Padova, Italy

P. Azzi^a, N. Bacchetta^a, D. Bisello^{a,b}, R. Carlin^{a,b}, P. Checchia^a, M. Dall'Osso^{a,b}, T. Dorigo^a, U. Dosselli^a, M. Galanti^{a,b}, U. Gasparini^{a,b}, A. Gozzelino^a, S. Lacaprara^a, M. Margoni^{a,b}, A.T. Meneguzzo^{a,b}, F. Montecassiano^a, M. Passaseo^a, J. Pazzini^{a,b}, M. Pegoraro^a, N. Pozzobon^{a,b}, P. Ronchese^{a,b}, F. Simonetto^{a,b}, E. Torassa^a, M. Tosi^{a,b}, S. Ventura^a, P. Zotto^{a,b}, A. Zucchetta^{a,b}

INFN Sezione di Pavia ^a, Università di Pavia ^b, Pavia, Italy

M. Gabusi^{a,b}, S.P. Ratti^{a,b}, V. Re^a, C. Riccardi^{a,b}, P. Salvini^a, P. Vitulo^{a,b}

INFN Sezione di Perugia ^a, Università di Perugia ^b, Perugia, Italy

M. Biasini^{a,b}, G.M. Bilei^a, D. Ciangottini^{a,b,2}, L. Fanò^{a,b}, P. Lariccia^{a,b}, G. Mantovani^{a,b}, M. Menichelli^a, A. Saha^a, A. Santocchia^{a,b}, A. Spiezia^{a,b,2}

INFN Sezione di Pisa ^a, Università di Pisa ^b, Scuola Normale Superiore di Pisa ^c, Pisa, Italy

K. Androsov^{a,25}, P. Azzurri^a, G. Bagliesi^a, J. Bernardini^a, T. Boccali^a, G. Broccolo^{a,c}, R. Castaldi^a, M.A. Ciocci^{a,25}, R. Dell'Orso^a, S. Donato^{a,c,2}, G. Fedi, F. Fiori^{a,c}, L. Foà^{a,c}, A. Giassi^a, M.T. Grippo^{a,25}, F. Ligabue^{a,c}, T. Lomtadze^a, L. Martini^{a,b}, A. Messineo^{a,b}, C.S. Moon^{a,26}, F. Palla^{a,2}, A. Rizzi^{a,b}, A. Savoy-Navarro^{a,27}, A.T. Serban^a, P. Spagnolo^a, P. Squillacioti^{a,25}, R. Tenchini^a, G. Tonelli^{a,b}, A. Venturi^a, P.G. Verdini^a, C. Vernieri^{a,c}

INFN Sezione di Roma ^a, Università di Roma ^b, Roma, Italy

L. Barone^{a,b}, F. Cavallari^a, G. D'imperio^{a,b}, D. Del Re^{a,b}, M. Diemoz^a, C. Jorda^a, E. Longo^{a,b}, F. Margaroli^{a,b}, P. Meridiani^a, F. Micheli^{a,b,2}, G. Organtini^{a,b}, R. Paramatti^a, S. Rahatlou^{a,b}, C. Rovelli^a, F. Santanastasio^{a,b}, L. Soffi^{a,b}, P. Traczyk^{a,b,2}

INFN Sezione di Torino ^a, Università di Torino ^b, Università del Piemonte Orientale (Novara) ^c, Torino, Italy

N. Amapane^{a,b}, R. Arcidiacono^{a,c}, S. Argiro^{a,b}, M. Arneodo^{a,c}, R. Bellan^{a,b}, C. Biino^a, N. Cartiglia^a, S. Casasso^{a,b,2}, M. Costa^{a,b}, A. Degano^{a,b}, N. Demaria^a, L. Finco^{a,b,2}, C. Mariotti^a, S. Maselli^a, E. Migliore^{a,b}, V. Monaco^{a,b}, M. Musich^a, M.M. Obertino^{a,c}, L. Pacher^{a,b}, N. Pastrone^a, M. Pelliccioni^a, G.L. Pinna Angioni^{a,b}, A. Potenza^{a,b}, A. Romero^{a,b}, M. Ruspa^{a,c}, R. Sacchi^{a,b}, A. Solano^{a,b}, A. Staiano^a, U. Tamponi^a

INFN Sezione di Trieste ^a, Università di Trieste ^b, Trieste, Italy

S. Belforte^a, V. Candelise^{a,b,2}, M. Casarsa^a, F. Cossutti^a, G. Della Ricca^{a,b}, B. Gobbo^a, C. La Licata^{a,b}, M. Marone^{a,b}, A. Schizzi^{a,b}, T. Umer^{a,b}, A. Zanetti^a

Kangwon National University, Chunchon, Korea

S. Chang, A. Kropivnitskaya, S.K. Nam

Kyungpook National University, Daegu, Korea

D.H. Kim, G.N. Kim, M.S. Kim, D.J. Kong, S. Lee, Y.D. Oh, H. Park, A. Sakharov, D.C. Son

Chonbuk National University, Jeonju, Korea

T.J. Kim, M.S. Ryu

Chonnam National University, Institute for Universe and Elementary Particles, Kwangju, Korea

J.Y. Kim, D.H. Moon, S. Song

Korea University, Seoul, Korea

S. Choi, D. Gyun, B. Hong, M. Jo, H. Kim, Y. Kim, B. Lee, K.S. Lee, S.K. Park, Y. Roh

Seoul National University, Seoul, Korea

H.D. Yoo

University of Seoul, Seoul, Korea

M. Choi, J.H. Kim, I.C. Park, G. Ryu

Sungkyunkwan University, Suwon, Korea

Y. Choi, Y.K. Choi, J. Goh, D. Kim, E. Kwon, J. Lee, I. Yu

Vilnius University, Vilnius, Lithuania

A. Juodagalvis

National Centre for Particle Physics, Universiti Malaya, Kuala Lumpur, Malaysia

J.R. Komaragiri, M.A.B. Md Ali

Centro de Investigacion y de Estudios Avanzados del IPN, Mexico City, Mexico

E. Casimiro Linares, H. Castilla-Valdez, E. De La Cruz-Burelo, I. Heredia-de La Cruz, A. Hernandez-Almada, R. Lopez-Fernandez, A. Sanchez-Hernandez

Universidad Iberoamericana, Mexico City, Mexico

S. Carrillo Moreno, F. Vazquez Valencia

Benemerita Universidad Autonoma de Puebla, Puebla, Mexico

I. Pedraza, H.A. Salazar Ibarguen

Universidad Autónoma de San Luis Potosí, San Luis Potosí, Mexico

A. Morelos Pineda

University of Auckland, Auckland, New Zealand

D. Krofcheck

University of Canterbury, Christchurch, New Zealand

P.H. Butler, S. Reucroft

National Centre for Physics, Quaid-I-Azam University, Islamabad, Pakistan

A. Ahmad, M. Ahmad, Q. Hassan, H.R. Hoorani, W.A. Khan, T. Khurshid, M. Shoaib

National Centre for Nuclear Research, Swierk, Poland

H. Bialkowska, M. Bluj, B. Boimska, T. Frueboes, M. Górski, M. Kazana, K. Nawrocki, K. Romanowska-Rybinska, M. Szleper, P. Zalewski

Institute of Experimental Physics, Faculty of Physics, University of Warsaw, Warsaw, Poland

G. Brona, K. Bunkowski, M. Cwiok, W. Dominik, K. Doroba, A. Kalinowski, M. Konecki, J. Krolikowski, M. Misiura, M. Olszewski

Laboratório de Instrumentação e Física Experimental de Partículas, Lisboa, Portugal

P. Bargassa, C. Beirão Da Cruz E Silva, P. Faccioli, P.G. Ferreira Parracho, M. Gallinaro, L. Lloret Iglesias, F. Nguyen, J. Rodrigues Antunes, J. Seixas, J. Varela, P. Vischia

Joint Institute for Nuclear Research, Dubna, Russia

S. Afanasiev, M. Gavrilenko, I. Golutvin, V. Karjavin, V. Konoplyanikov, V. Korenkov, A. Lanev, A. Malakhov, V. Matveev²⁸, V.V. Mitsyn, P. Moisezenz, V. Palichik, V. Perelygin, S. Shmatov, N. Skatchkov, V. Smirnov, E. Tikhonenko, A. Zarubin

Petersburg Nuclear Physics Institute, Gatchina (St. Petersburg), Russia

V. Golovtsov, Y. Ivanov, V. Kim²⁹, E. Kuznetsova, P. Levchenko, V. Murzin, V. Oreshkin, I. Smirnov, V. Sulimov, L. Uvarov, S. Vavilov, A. Vorobyev, An. Vorobyev

Institute for Nuclear Research, Moscow, Russia

Yu. Andreev, A. Dermenev, S. Gninenko, N. Golubev, M. Kirsanov, N. Krasnikov, A. Pashenkov, D. Tlisov, A. Toropin

Institute for Theoretical and Experimental Physics, Moscow, Russia

V. Epshteyn, V. Gavrilov, N. Lychkovskaya, V. Popov, I. Pozdnyakov, G. Safronov, S. Semenov, A. Spiridonov, V. Stolin, E. Vlasov, A. Zhokin

P.N. Lebedev Physical Institute, Moscow, Russia

V. Andreev, M. Azarkin³⁰, I. Dremin³⁰, M. Kirakosyan, A. Leonidov³⁰, G. Mesyats, S.V. Rusakov, A. Vinogradov

Skobeltsyn Institute of Nuclear Physics, Lomonosov Moscow State University, Moscow, Russia

A. Belyaev, E. Boos, M. Dubinin³¹, L. Dudko, A. Ershov, A. Gribushin, V. Klyukhin, O. Kodolova, I. Lokhtin, S. Obraztsov, S. Petrushanko, V. Savrin, A. Snigirev

State Research Center of Russian Federation, Institute for High Energy Physics, Protvino, Russia

I. Azhgirey, I. Bayshev, S. Bitioukov, V. Kachanov, A. Kalinin, D. Konstantinov, V. Krychkine, V. Petrov, R. Ryutin, A. Sobol, L. Tourtchanovitch, S. Troshin, N. Tyurin, A. Uzunian, A. Volkov

University of Belgrade, Faculty of Physics and Vinca Institute of Nuclear Sciences, Belgrade, Serbia

P. Adzic³², M. Ekmedzic, J. Milosevic, V. Rekovic

Centro de Investigaciones Energéticas Medioambientales y Tecnológicas (CIEMAT), Madrid, Spain

J. Alcaraz Maestre, C. Battilana, E. Calvo, M. Cerrada, M. Chamizo Llatas, N. Colino, B. De La Cruz, A. Delgado Peris, D. Domínguez Vázquez, A. Escalante Del Valle, C. Fernandez Bedoya, J.P. Fernández Ramos, J. Flix, M.C. Fouz, P. Garcia-Abia, O. Gonzalez Lopez, S. Goy Lopez, J.M. Hernandez, M.I. Josa, E. Navarro De Martino, A. Pérez-Calero Yzquierdo, J. Puerta Pelayo, A. Quintario Olmeda, I. Redondo, L. Romero, M.S. Soares

Universidad Autónoma de Madrid, Madrid, Spain

C. Albajar, J.F. de Trocóniz, M. Missiroli, D. Moran

Universidad de Oviedo, Oviedo, Spain

H. Brun, J. Cuevas, J. Fernandez Menendez, S. Folgueras, I. Gonzalez Caballero

Instituto de Física de Cantabria (IFCA), CSIC-Universidad de Cantabria, Santander, Spain

J.A. Brochero Cifuentes, I.J. Cabrillo, A. Calderon, J. Duarte Campderros, M. Fernandez, G. Gomez, A. Graziano, A. Lopez Virto, J. Marco, R. Marco, C. Martinez Rivero, F. Matorras, F.J. Munoz Sanchez, J. Piedra Gomez, T. Rodrigo, A.Y. Rodríguez-Marrero, A. Ruiz-Jimeno, L. Scodellaro, I. Vila, R. Vilar Cortabitarte

CERN, European Organization for Nuclear Research, Geneva, Switzerland

D. Abbaneo, E. Auffray, G. Auzinger, M. Bachtis, P. Baillon, A.H. Ball, D. Barney, A. Benaglia, J. Bendavid, L. Benhabib, J.F. Benitez, P. Bloch, A. Bocci, A. Bonato, O. Bondu, C. Botta, H. Breuker, T. Camporesi, G. Cerminara, S. Colafranceschi³³, M. D'Alfonso, D. d'Enterria, A. Dabrowski, A. David, F. De Guio, A. De Roeck, S. De Visscher, E. Di Marco, M. Dobson, M. Dordevic, B. Dorney, N. Dupont-Sagorin, A. Elliott-Peisert, G. Franzoni, W. Funk, D. Gigi, K. Gill, D. Giordano, M. Girone, F. Glege, R. Guida, S. Gundacker, M. Guthoff, J. Hammer, M. Hansen, P. Harris, J. Hegeman, V. Innocente, P. Janot, K. Kousouris, K. Krajczar, P. Lecoq,

C. Lourenço, N. Magini, L. Malgeri, M. Mannelli, J. Marrouche, L. Masetti, F. Meijers, S. Mersi, E. Meschi, F. Moortgat, S. Morovic, M. Mulders, L. Orsini, L. Pape, E. Perez, A. Petrilli, G. Petrucciani, A. Pfeiffer, M. Pimiä, D. Piparo, M. Plagge, A. Racz, G. Rolandi³⁴, M. Rovere, H. Sakulin, C. Schäfer, C. Schwick, A. Sharma, P. Siegrist, P. Silva, M. Simon, P. Sphicas³⁵, D. Spiga, J. Steggemann, B. Stieger, M. Stoye, Y. Takahashi, D. Treille, A. Tsirou, G.I. Veres¹⁷, N. Wardle, H.K. Wöhri, H. Wollny, W.D. Zeuner

Paul Scherrer Institut, Villigen, Switzerland

W. Bertl, K. Deiters, W. Erdmann, R. Horisberger, Q. Ingram, H.C. Kaestli, D. Kotlinski, U. Langenegger, D. Renker, T. Rohe

Institute for Particle Physics, ETH Zurich, Zurich, Switzerland

F. Bachmair, L. Bäni, L. Bianchini, M.A. Buchmann, B. Casal, N. Chanon, G. Dissertori, M. Dittmar, M. Donegà, M. Dünser, P. Eller, C. Grab, D. Hits, J. Hoss, W. Luster, M. Mangano, A.C. Marini, M. Marionneau, P. Martinez Ruiz del Arbol, M. Masciovecchio, D. Meister, N. Mohr, P. Musella, C. Nägeli³⁶, F. Nessi-Tedaldi, F. Pandolfi, F. Pauss, L. Perrozzi, M. Peruzzi, M. Quittnat, L. Rebane, M. Rossini, A. Starodumov³⁷, M. Takahashi, K. Theofilatos, R. Wallny, H.A. Weber

Universität Zürich, Zurich, Switzerland

C. Amsler³⁸, M.F. Canelli, V. Chiochia, A. De Cosa, A. Hinzmann, T. Hreus, B. Kilminster, C. Lange, B. Millan Mejias, J. Ngadiuba, D. Pinna, P. Robmann, F.J. Ronga, S. Taroni, M. Verzetti, Y. Yang

National Central University, Chung-Li, Taiwan

M. Cardaci, K.H. Chen, C. Ferro, C.M. Kuo, W. Lin, Y.J. Lu, R. Volpe, S.S. Yu

National Taiwan University (NTU), Taipei, Taiwan

P. Chang, Y.H. Chang, Y. Chao, K.F. Chen, P.H. Chen, C. Dietz, U. Grundler, W.-S. Hou, Y.F. Liu, R.-S. Lu, E. Petrakou, Y.M. Tzeng, R. Wilken

Chulalongkorn University, Faculty of Science, Department of Physics, Bangkok, Thailand

B. Asavapibhop, G. Singh, N. Srimanobhas, N. Suwonjandee

Cukurova University, Adana, Turkey

A. Adiguzel, M.N. Bakirci³⁹, S. Cerci⁴⁰, C. Dozen, I. Dumanoglu, E. Eskut, S. Girgis, G. Gokbulut, Y. Guler, E. Gurpinar, I. Hos, E.E. Kangal, A. Kayis Topaksu, G. Onengut⁴¹, K. Ozdemir, S. Ozturk³⁹, A. Polatoz, D. Sunar Cerci⁴⁰, B. Tali⁴⁰, H. Topakli³⁹, M. Vergili, C. Zorbilmez

Middle East Technical University, Physics Department, Ankara, Turkey

I.V. Akin, B. Bilin, S. Bilmis, H. Gamsizkan⁴², B. Isildak⁴³, G. Karapinar⁴⁴, K. Ocalan⁴⁵, S. Sekmen, U.E. Surat, M. Yalvac, M. Zeyrek

Bogazici University, Istanbul, Turkey

E.A. Albayrak⁴⁶, E. Gülmez, M. Kaya⁴⁷, O. Kaya⁴⁸, T. Yetkin⁴⁹

Istanbul Technical University, Istanbul, Turkey

K. Cankocak, F.I. Vardarli

National Scientific Center, Kharkov Institute of Physics and Technology, Kharkov, Ukraine

L. Levchuk, P. Sorokin

University of Bristol, Bristol, United Kingdom

J.J. Brooke, E. Clement, D. Cussans, H. Flacher, J. Goldstein, M. Grimes, G.P. Heath, H.F. Heath,

J. Jacob, L. Kreczko, C. Lucas, Z. Meng, D.M. Newbold⁵⁰, S. Paramesvaran, A. Poll, T. Sakuma, S. Seif El Nasr-storey, S. Senkin, V.J. Smith

Rutherford Appleton Laboratory, Didcot, United Kingdom

K.W. Bell, A. Belyaev⁵¹, C. Brew, R.M. Brown, D.J.A. Cockerill, J.A. Coughlan, K. Harder, S. Harper, E. Olaiya, D. Petyt, C.H. Shepherd-Themistocleous, A. Thea, I.R. Tomalin, T. Williams, W.J. Womersley, S.D. Worm

Imperial College, London, United Kingdom

M. Baber, R. Bainbridge, O. Buchmuller, D. Burton, D. Colling, N. Cripps, P. Dauncey, G. Davies, M. Della Negra, P. Dunne, W. Ferguson, J. Fulcher, D. Futyan, G. Hall, G. Iles, M. Jarvis, G. Karapostoli, M. Kenzie, R. Lane, R. Lucas⁵⁰, L. Lyons, A.-M. Magnan, S. Malik, B. Mathias, J. Nash, A. Nikitenko³⁷, J. Pela, M. Pesaresi, K. Petridis, D.M. Raymond, S. Rogerson, A. Rose, C. Seez, P. Sharp[†], A. Tapper, M. Vazquez Acosta, T. Virdee, S.C. Zenz

Brunel University, Uxbridge, United Kingdom

J.E. Cole, P.R. Hobson, A. Khan, P. Kyberd, D. Leggat, D. Leslie, I.D. Reid, P. Symonds, L. Teodorescu, M. Turner

Baylor University, Waco, USA

J. Dittmann, K. Hatakeyama, A. Kasmi, H. Liu, T. Scarborough, Z. Wu

The University of Alabama, Tuscaloosa, USA

O. Charaf, S.I. Cooper, C. Henderson, P. Rumerio

Boston University, Boston, USA

A. Avetisyan, T. Bose, C. Fantasia, P. Lawson, C. Richardson, J. Rohlf, J. St. John, L. Sulak

Brown University, Providence, USA

J. Alimena, E. Berry, S. Bhattacharya, G. Christopher, D. Cutts, Z. Demiragli, N. Dhingra, A. Ferapontov, A. Garabedian, U. Heintz, G. Kukartsev, E. Laird, G. Landsberg, M. Luk, M. Narain, M. Segala, T. Sinthuprasith, T. Speer, J. Swanson

University of California, Davis, Davis, USA

R. Breedon, G. Breto, M. Calderon De La Barca Sanchez, S. Chauhan, M. Chertok, J. Conway, R. Conway, P.T. Cox, R. Erbacher, M. Gardner, W. Ko, R. Lander, M. Mulhearn, D. Pellett, J. Pilot, F. Ricci-Tam, S. Shalhout, J. Smith, M. Squires, D. Stolp, M. Tripathi, S. Wilbur, R. Yohay

University of California, Los Angeles, USA

R. Cousins, P. Everaerts, C. Farrell, J. Hauser, M. Ignatenko, G. Rakness, E. Takasugi, V. Valuev, M. Weber

University of California, Riverside, Riverside, USA

K. Burt, R. Clare, J. Ellison, J.W. Gary, G. Hanson, J. Heilman, M. Ivova Rikova, P. Jandir, E. Kennedy, F. Lacroix, O.R. Long, A. Luthra, M. Malberti, M. Olmedo Negrete, A. Shrinivas, S. Sumowidagdo, S. Wimpenny

University of California, San Diego, La Jolla, USA

J.G. Branson, G.B. Cerati, S. Cittolin, R.T. D'Agnolo, A. Holzner, R. Kelley, D. Klein, J. Letts, I. Macneill, D. Olivito, S. Padhi, C. Palmer, M. Pieri, M. Sani, V. Sharma, S. Simon, M. Tadel, Y. Tu, A. Vartak, C. Welke, F. Würthwein, A. Yagil

University of California, Santa Barbara, Santa Barbara, USA

D. Barge, J. Bradmiller-Feld, C. Campagnari, T. Danielson, A. Dishaw, V. Dutta, K. Flowers,

M. Franco Sevilla, P. Geffert, C. George, F. Golf, L. Gouskos, J. Incandela, C. Justus, N. Mccoll, J. Richman, D. Stuart, W. To, C. West, J. Yoo

California Institute of Technology, Pasadena, USA

A. Apresyan, A. Bornheim, J. Bunn, Y. Chen, J. Duarte, A. Mott, H.B. Newman, C. Pena, M. Pierini, M. Spiropulu, J.R. Vlimant, R. Wilkinson, S. Xie, R.Y. Zhu

Carnegie Mellon University, Pittsburgh, USA

V. Azzolini, A. Calamba, B. Carlson, T. Ferguson, Y. Iiyama, M. Paulini, J. Russ, H. Vogel, I. Vorobiev

University of Colorado at Boulder, Boulder, USA

J.P. Cumalat, W.T. Ford, A. Gaz, M. Krohn, E. Luiggi Lopez, U. Nauenberg, J.G. Smith, K. Stenson, S.R. Wagner

Cornell University, Ithaca, USA

J. Alexander, A. Chatterjee, J. Chaves, J. Chu, S. Dittmer, N. Eggert, N. Mirman, G. Nicolas Kaufman, J.R. Patterson, A. Ryd, E. Salvati, L. Skinnari, W. Sun, W.D. Teo, J. Thom, J. Thompson, J. Tucker, Y. Weng, L. Winstrom, P. Wittich

Fairfield University, Fairfield, USA

D. Winn

Fermi National Accelerator Laboratory, Batavia, USA

S. Abdullin, M. Albrow, J. Anderson, G. Apollinari, L.A.T. Bauerdick, A. Beretvas, J. Berryhill, P.C. Bhat, G. Bolla, K. Burkett, J.N. Butler, H.W.K. Cheung, F. Chlebana, S. Cihangir, V.D. Elvira, I. Fisk, J. Freeman, E. Gottschalk, L. Gray, D. Green, S. Grünendahl, O. Gutsche, J. Hanlon, D. Hare, R.M. Harris, J. Hirschauer, B. Hooberman, S. Jindariani, M. Johnson, U. Joshi, B. Klima, B. Kreis, S. Kwan[†], J. Linacre, D. Lincoln, R. Lipton, T. Liu, J. Lykken, K. Maeshima, J.M. Marraffino, V.I. Martinez Outschoorn, S. Maruyama, D. Mason, P. McBride, P. Merkel, K. Mishra, S. Mrenna, S. Nahn, C. Newman-Holmes, V. O'Dell, O. Prokofyev, E. Sexton-Kennedy, S. Sharma, A. Soha, W.J. Spalding, L. Spiegel, L. Taylor, S. Tkaczyk, N.V. Tran, L. Uplegger, E.W. Vaandering, R. Vidal, A. Whitbeck, J. Whitmore, F. Yang

University of Florida, Gainesville, USA

D. Acosta, P. Avery, P. Bortignon, D. Bourilkov, M. Carver, D. Curry, S. Das, M. De Gruttola, G.P. Di Giovanni, R.D. Field, M. Fisher, I.K. Furic, J. Hugon, J. Konigsberg, A. Korytov, T. Kypreos, J.F. Low, K. Matchev, H. Mei, P. Milenovic⁵², G. Mitselmakher, L. Muniz, A. Rinkevicius, L. Shchutska, M. Snowball, D. Sperka, J. Yelton, M. Zakaria

Florida International University, Miami, USA

S. Hewamanage, S. Linn, P. Markowitz, G. Martinez, J.L. Rodriguez

Florida State University, Tallahassee, USA

T. Adams, A. Askew, J. Bochenek, B. Diamond, J. Haas, S. Hagopian, V. Hagopian, K.F. Johnson, H. Prosper, V. Veeraraghavan, M. Weinberg

Florida Institute of Technology, Melbourne, USA

M.M. Baarmand, M. Hohlmann, H. Kalakhety, F. Yumiceva

University of Illinois at Chicago (UIC), Chicago, USA

M.R. Adams, L. Apanasevich, D. Berry, R.R. Betts, I. Bucinskaite, R. Cavanaugh, O. Evdokimov, L. Gauthier, C.E. Gerber, D.J. Hofman, P. Kurt, C. O'Brien, I.D. Sandoval Gonzalez, C. Silkworth, P. Turner, N. Varelas

The University of Iowa, Iowa City, USA

B. Bilki⁵³, W. Clarida, K. Dilsiz, M. Haytmyradov, J.-P. Merlo, H. Mermerkaya⁵⁴, A. Mestvirishvili, A. Moeller, J. Nachtman, H. Ogul, Y. Onel, F. Ozok⁴⁶, A. Penzo, R. Rahmat, S. Sen, P. Tan, E. Tiras, J. Wetzel, K. Yi

Johns Hopkins University, Baltimore, USA

I. Anderson, B.A. Barnett, B. Blumenfeld, S. Bolognesi, D. Fehling, A.V. Gritsan, P. Maksimovic, C. Martin, M. Swartz

The University of Kansas, Lawrence, USA

P. Baringer, A. Bean, G. Benelli, C. Bruner, J. Gray, R.P. Kenny III, D. Majumder, M. Malek, M. Murray, D. Noonan, S. Sanders, J. Sekaric, R. Stringer, Q. Wang, J.S. Wood

Kansas State University, Manhattan, USA

I. Chakaberia, A. Ivanov, K. Kaadze, S. Khalil, M. Makouski, Y. Maravin, L.K. Saini, N. Skhirtladze, I. Svintradze

Lawrence Livermore National Laboratory, Livermore, USA

J. Gronberg, D. Lange, F. Rebassoo, D. Wright

University of Maryland, College Park, USA

A. Baden, A. Belloni, B. Calvert, S.C. Eno, J.A. Gomez, N.J. Hadley, R.G. Kellogg, T. Kolberg, Y. Lu, A.C. Mignerey, K. Pedro, A. Skuja, M.B. Tonjes, S.C. Tonwar

Massachusetts Institute of Technology, Cambridge, USA

A. Apyan, R. Barbieri, W. Busza, I.A. Cali, M. Chan, L. Di Matteo, G. Gomez Ceballos, M. Goncharov, D. Gulhan, M. Klute, Y.S. Lai, Y.-J. Lee, A. Levin, P.D. Luckey, C. Paus, D. Ralph, C. Roland, G. Roland, G.S.F. Stephans, K. Sumorok, D. Velicanu, J. Veverka, B. Wyslouch, M. Yang, M. Zanetti, V. Zhukova

University of Minnesota, Minneapolis, USA

B. Dahmes, A. Gude, S.C. Kao, K. Klapoetke, Y. Kubota, J. Mans, S. Nourbakhsh, N. Pastika, R. Rusack, A. Singovsky, N. Tambe, J. Turkewitz

University of Mississippi, Oxford, USA

J.G. Acosta, S. Oliveros

University of Nebraska-Lincoln, Lincoln, USA

E. Avdeeva, K. Bloom, S. Bose, D.R. Claes, A. Dominguez, R. Gonzalez Suarez, J. Keller, D. Knowlton, I. Kravchenko, J. Lazo-Flores, F. Meier, F. Ratnikov, G.R. Snow, M. Zvada

State University of New York at Buffalo, Buffalo, USA

J. Dolen, A. Godshalk, I. Iashvili, A. Kharchilava, A. Kumar, S. Rappoccio

Northeastern University, Boston, USA

G. Alverson, E. Barberis, D. Baumgartel, M. Chasco, A. Massironi, D.M. Morse, D. Nash, T. Orimoto, D. Trocino, R.-J. Wang, D. Wood, J. Zhang

Northwestern University, Evanston, USA

K.A. Hahn, A. Kubik, N. Mucia, N. Odell, B. Pollack, A. Pozdnyakov, M. Schmitt, S. Stoynev, K. Sung, M. Velasco, S. Won

University of Notre Dame, Notre Dame, USA

A. Brinkerhoff, K.M. Chan, A. Drozdetskiy, M. Hildreth, C. Jessop, D.J. Karmgard, N. Kellams, K. Lannon, S. Lynch, N. Marinelli, Y. Musienko²⁸, T. Pearson, M. Planer, R. Ruchti, G. Smith, N. Valls, M. Wayne, M. Wolf, A. Woodard

The Ohio State University, Columbus, USA

L. Antonelli, J. Brinson, B. Bylsma, L.S. Durkin, S. Flowers, A. Hart, C. Hill, R. Hughes, K. Kotov, T.Y. Ling, W. Luo, D. Puigh, M. Rodenburg, B.L. Winer, H. Wolfe, H.W. Wulsin

Princeton University, Princeton, USA

O. Driga, P. Elmer, J. Hardenbrook, P. Hebda, S.A. Koay, P. Lujan, D. Marlow, T. Medvedeva, M. Mooney, J. Olsen, P. Piroué, X. Quan, H. Saka, D. Stickland², C. Tully, J.S. Werner, A. Zuranski

University of Puerto Rico, Mayaguez, USA

E. Brownson, S. Malik, H. Mendez, J.E. Ramirez Vargas

Purdue University, West Lafayette, USA

V.E. Barnes, D. Benedetti, D. Bortoletto, M. De Mattia, L. Gutay, Z. Hu, M.K. Jha, M. Jones, K. Jung, M. Kress, N. Leonardo, D.H. Miller, N. Neumeister, B.C. Radburn-Smith, X. Shi, I. Shipsey, D. Silvers, A. Svyatkovskiy, F. Wang, W. Xie, L. Xu, J. Zablocki

Purdue University Calumet, Hammond, USA

N. Parashar, J. Stupak

Rice University, Houston, USA

A. Adair, B. Akgun, K.M. Ecklund, F.J.M. Geurts, W. Li, B. Michlin, B.P. Padley, R. Redjimi, J. Roberts, J. Zabel

University of Rochester, Rochester, USA

B. Betchart, A. Bodek, R. Covarelli, P. de Barbaro, R. Demina, Y. Eshaq, T. Ferbel, A. Garcia-Bellido, P. Goldenzweig, J. Han, A. Harel, O. Hindrichs, A. Khukhunaishvili, S. Korjenevski, G. Petrillo, D. Vishnevskiy

The Rockefeller University, New York, USA

R. Ciesielski, L. Demortier, K. Goulianos, C. Mesropian

Rutgers, The State University of New Jersey, Piscataway, USA

S. Arora, A. Barker, J.P. Chou, C. Contreras-Campana, E. Contreras-Campana, D. Duggan, D. Ferencek, Y. Gershtein, R. Gray, E. Halkiadakis, D. Hidas, S. Kaplan, A. Lath, S. Panwalkar, M. Park, R. Patel, S. Salur, S. Schnetzer, D. Sheffield, S. Somalwar, R. Stone, S. Thomas, P. Thomassen, M. Walker

University of Tennessee, Knoxville, USA

K. Rose, S. Spanier, A. York

Texas A&M University, College Station, USA

O. Bouhali⁵⁵, A. Castaneda Hernandez, R. Eusebi, W. Flanagan, J. Gilmore, T. Kamon⁵⁶, V. Khotilovich, V. Krutelyov, R. Montalvo, I. Osipenkov, Y. Pakhotin, A. Perloff, J. Roe, A. Rose, A. Safonov, I. Suarez, A. Tatarinov, K.A. Ulmer

Texas Tech University, Lubbock, USA

N. Akchurin, C. Cowden, J. Damgov, C. Dragoiu, P.R. Duderu, J. Faulkner, K. Kovitangoon, S. Kunori, S.W. Lee, T. Libeiro, I. Volobouev

Vanderbilt University, Nashville, USA

E. Appelt, A.G. Delannoy, S. Greene, A. Gurrola, W. Johns, C. Maguire, Y. Mao, A. Melo, M. Sharma, P. Sheldon, B. Snook, S. Tuo, J. Velkovska

University of Virginia, Charlottesville, USA

M.W. Arenton, S. Boutle, B. Cox, B. Francis, J. Goodell, R. Hirosky, A. Ledovskoy, H. Li, C. Lin, C. Neu, J. Wood

Wayne State University, Detroit, USA

C. Clarke, R. Harr, P.E. Karchin, C. Kottachchi Kankanamge Don, P. Lamichhane, J. Sturdy

University of Wisconsin, Madison, USA

D.A. Belknap, D. Carlsmith, M. Cepeda, S. Dasu, L. Dodd, S. Duric, E. Friis, R. Hall-Wilton, M. Herndon, A. Hervé, P. Klabbers, A. Lanaro, C. Lazaridis, A. Levine, R. Loveless, A. Mohapatra, I. Ojalvo, T. Perry, G.A. Pierro, G. Polese, I. Ross, T. Sarangi, A. Savin, W.H. Smith, D. Taylor, C. Vuosalo, N. Woods

†: Deceased

- 1: Also at Vienna University of Technology, Vienna, Austria
- 2: Also at CERN, European Organization for Nuclear Research, Geneva, Switzerland
- 3: Also at Institut Pluridisciplinaire Hubert Curien, Université de Strasbourg, Université de Haute Alsace Mulhouse, CNRS/IN2P3, Strasbourg, France
- 4: Also at National Institute of Chemical Physics and Biophysics, Tallinn, Estonia
- 5: Also at Skobeltsyn Institute of Nuclear Physics, Lomonosov Moscow State University, Moscow, Russia
- 6: Also at Universidade Estadual de Campinas, Campinas, Brazil
- 7: Also at Laboratoire Leprince-Ringuet, Ecole Polytechnique, IN2P3-CNRS, Palaiseau, France
- 8: Also at Joint Institute for Nuclear Research, Dubna, Russia
- 9: Also at Suez University, Suez, Egypt
- 10: Also at Cairo University, Cairo, Egypt
- 11: Also at Fayoum University, El-Fayoum, Egypt
- 12: Also at British University in Egypt, Cairo, Egypt
- 13: Now at Ain Shams University, Cairo, Egypt
- 14: Also at Université de Haute Alsace, Mulhouse, France
- 15: Also at Brandenburg University of Technology, Cottbus, Germany
- 16: Also at Institute of Nuclear Research ATOMKI, Debrecen, Hungary
- 17: Also at Eötvös Loránd University, Budapest, Hungary
- 18: Also at University of Debrecen, Debrecen, Hungary
- 19: Also at University of Visva-Bharati, Santiniketan, India
- 20: Now at King Abdulaziz University, Jeddah, Saudi Arabia
- 21: Also at University of Ruhuna, Matara, Sri Lanka
- 22: Also at Isfahan University of Technology, Isfahan, Iran
- 23: Also at University of Tehran, Department of Engineering Science, Tehran, Iran
- 24: Also at Plasma Physics Research Center, Science and Research Branch, Islamic Azad University, Tehran, Iran
- 25: Also at Università degli Studi di Siena, Siena, Italy
- 26: Also at Centre National de la Recherche Scientifique (CNRS) - IN2P3, Paris, France
- 27: Also at Purdue University, West Lafayette, USA
- 28: Also at Institute for Nuclear Research, Moscow, Russia
- 29: Also at St. Petersburg State Polytechnical University, St. Petersburg, Russia
- 30: Also at National Research Nuclear University 'Moscow Engineering Physics Institute' (MEPhI), Moscow, Russia
- 31: Also at California Institute of Technology, Pasadena, USA
- 32: Also at Faculty of Physics, University of Belgrade, Belgrade, Serbia
- 33: Also at Facoltà Ingegneria, Università di Roma, Roma, Italy

-
- 34: Also at Scuola Normale e Sezione dell'INFN, Pisa, Italy
 - 35: Also at University of Athens, Athens, Greece
 - 36: Also at Paul Scherrer Institut, Villigen, Switzerland
 - 37: Also at Institute for Theoretical and Experimental Physics, Moscow, Russia
 - 38: Also at Albert Einstein Center for Fundamental Physics, Bern, Switzerland
 - 39: Also at Gaziosmanpasa University, Tokat, Turkey
 - 40: Also at Adiyaman University, Adiyaman, Turkey
 - 41: Also at Cag University, Mersin, Turkey
 - 42: Also at Anadolu University, Eskisehir, Turkey
 - 43: Also at Ozyegin University, Istanbul, Turkey
 - 44: Also at Izmir Institute of Technology, Izmir, Turkey
 - 45: Also at Necmettin Erbakan University, Konya, Turkey
 - 46: Also at Mimar Sinan University, Istanbul, Istanbul, Turkey
 - 47: Also at Marmara University, Istanbul, Turkey
 - 48: Also at Kafkas University, Kars, Turkey
 - 49: Also at Yildiz Technical University, Istanbul, Turkey
 - 50: Also at Rutherford Appleton Laboratory, Didcot, United Kingdom
 - 51: Also at School of Physics and Astronomy, University of Southampton, Southampton, United Kingdom
 - 52: Also at University of Belgrade, Faculty of Physics and Vinca Institute of Nuclear Sciences, Belgrade, Serbia
 - 53: Also at Argonne National Laboratory, Argonne, USA
 - 54: Also at Erzincan University, Erzincan, Turkey
 - 55: Also at Texas A&M University at Qatar, Doha, Qatar
 - 56: Also at Kyungpook National University, Daegu, Korea